Preparation, Structure, and Properties of Pseudotetrahedral, D_{2d} Complexes of Cu(II), Ni(II), Co(II), Cu(I), and Zn(II) with the Geometrically Constraining Bidentate Ligand 2,2'-Bis(2-imidazolyl)biphenyl. Examination of Electron Self-Exchange for the Cu(I)/Cu(II) Pair

Spencer Knapp,* Terence P. Keenan, Xiaohua Zhang, Ronald Fikar, Joseph A. Potenza,* and Harvey J. Schugar*

Contribution from the Department of Chemistry, Rutgers, The State University of New Jersey, New Brunswick, New Jersey 08903. *Received September 5, 1989*

Abstract: The bidentate ligand 2,2'-bis(2-imidazolyl)biphenyl (3 = L) has been synthesized and used to prepare perchlorate complexes containing Cu(II) (**5**), Ni(II) (**6**), Co(II) (**7**), Cu(I) (**8**), and Zn(II). X-ray structure analysis of **5**–**8** reveals pseudotetrahedral, $MN(imH)_4$ chromophores, each with approximate D_{2d} point symmetry. The ligand **3** exerts an unprecedented degree of geometric control of the coordination spheres for complexes of this type. In **5**–**8**, the MN_2/MN'_2 dihedral angles range from 87.2 (2) to 89.5 (1)° and are close to the ideal, tetrahedral value (90°). D_{2d} flattening of the coordination sphere is greatest in the Cu(II) complex, followed by the Ni(II), Co(II), and Cu(I) complexes. Geometric constraints within the nine-membered chelate rings cause intraligand N–M–N angles to exceed the tetrahedral value, flattening the otherwise tetrahedral MN_4 units; additional ligand field effects result in still larger angles for the Cu(II) and Ni(II) species. Electrochemical measurements for the CuL_2^+/CuL_2^{2+} couple in acetonitrile revealed a reversible redox reaction at a scan rate of 50 mV s^{-1} with $E_{1/2}$ = +0.11 (1) V vs SSCE. NMR techniques were used to examine the rate of electron self-exchange for the pseudotetrahedral Cu(I)/Cu(II) pair in acetonitrile. ^1H T_1 and T^*_2 measurements showed that the self-exchange rate constant k is less than 10^2 M^{-1} s^{-1} over the −20 to +20 °C temperature range. This surprisingly small value may result from ineffective interaction of the unpaired electron in the Cu(II) complex with ligand orbitals. X-band EPR spectra for **5** and for the Cu(II)-doped $ZnL_2(ClO_4)_2$ complex are reported. Spectra of the latter closely resemble those of superoxide dismutase with Cu(II) doped into the tetrahedral Zn(II) site, and the half-met nitrite forms of hemocyanin and tyrosinase. UV–vis spectra of **5**–**8** are reported. An absorption band at 22 700 cm^{-1} in the Cu(II) complex **5**, assigned as π(imH) → Cu(II) LMCT, compares favorably in energy and intensity with the corresponding absorptions observed for plastocyanin and Cu(II)-doped Zn superoxide dismutase.

Nearly tetrahedral Cu(I)/Cu(II) model complexes that are well-defined, approximately isostructural, and that contain biologically relevant ligation can be used to probe important questions about the active sites of copper metalloproteins that embody this structural feature. For example, the factors that govern Cu(I)/Cu(II) electron self-exchange reactions for protein active sites are not well understood. The kinetic implications of low reorganization energies (along with electronic and other factors) could be explored by studies of suitable isostructural model Cu(I)/Cu(II) redox couples. The electronic structures of the reduced copper protein sites are poorly defined and could be probed by photoelectron spectroscopy studies[1,2] of suitable Cu(I) model complexes. Moreover, the charge-transfer and EPR spectra of the blue copper and other sites have yet to be modeled with other than tetragonal Cu(II) complexes or pseudotetrahedral complexes containing abiological ligation. To prepare more useful Cu(II) models, the ligand-field-driven distortion of biologically relevant Cu(II) complexes must be suppressed, and the redox instability of the Cu(II)–thiolate bond must be controlled.

Blue copper proteins, such as plastocyanin and azurin, are biological electron carriers. Their facile electron-transfer abilities have been linked to small barriers for active site inner-sphere reorganization for the Cu(I)/Cu(II) redox couple.[3,4] Protein crystallographic studies have revealed that the Cu(II) sites are elongated C_{3v} CuN_2SS^* units comprised of an approximately trigonal-planar $Cu(His)_2(Cys)$ unit additionally ligated by an apical methionine thioether (S*).[3,5,6] A glycine carbonyl oxygen atom is, in our view, too far removed (3.1 Å) from the Cu atom in azurin from *Alcaligenes denitrificans* for consideration as a second apical ligand.[6] For poplar plastocyanin, crystallographic studies have shown that reduction affords an almost isostructural $Cu^IN_2SS^*$ unit whose formation entails only minor rearrangements for the protein donor groups.[7] The observation that quite similar arrangements of the donor groups are present in Hg(II)-substituted and apoplastocyanin[8,9] suggests that the binding site geometry is fairly rigid and implies that the Cu(I)/Cu(II) redox couple is constrained by the protein to be nearly isostructural. It appears likely that this situation will also obtain for the azurins. Since elongated C_{3v} ("3 + 1") coordination is common for Cu(I),[10,11] the reduced active site geometries in the azurins can closely approximate those noted above for the Cu(II) sites. While these blue copper sites are expected to have relatively small reorganization energies, their rates of electron self-exchange vary significantly from $\ll 2 \times 10^4$ M^{-1} s^{-1} for French bean plastocyanin to 1.3×10^6 for *Pseudomonas aeruginosa* azurin.[12] Owing to the complicated nature of electron self-exchange for metalloproteins, it is not possible to determine how the rates of electron transfer may be influenced by the near invariance of the active site geometries to changes in valence state.

(1) Didziulis, S. V.; Cohen, S. L.; Butcher, K. D.; Solomon, E. I. *Inorg. Chem.* **1988**, *27*, 2238.
(2) Didziulis, S. V.; Cohen, S. L.; Gewirth, A. A.; Solomon, E. I. *J. Am. Chem. Soc.* **1988**, *110*, 250.
(3) Guss, J. M.; Freeman, H. C. *J. Mol. Biol.* **1983**, *169*, 521.
(4) Solomon, E. I.; Hare, J. W.; Dooley, D. M.; Dawson, J. H.; Stephens, P. J.; Gray, H. B. *J. Am. Chem. Soc.* **1980**, *102*, 168.
(5) Adman, E. T.; Stenkamp, R. E.; Sieker, L. C.; Jensen, L. H. *J. Mol. Biol.* **1978**, *123*, 35.
(6) Norris, G. E.; Anderson, B. F.; Baker, E. N. *J. Am. Chem. Soc.* **1986**, *108*, 2784.
(7) Guss, J. M.; Harrowell, P. R.; Murata, M.; Norris, V. A.; Freeman, H. C. *J. Mol. Biol.* **1986**, *192*, 361.
(8) Church, W. B.; Guss, J. M.; Potter, J. J.; Freeman, H. C. *J. Biol. Chem.* **1986**, *261*, 234.
(9) Garrett, T. P. J.; Clingeleffer, D. J.; Guss, J. M.; Rogers, S. J.; Freeman, H. C. *J. Biol. Chem.* **1984**, *259*, 2822.
(10) Schugar, H. J.; Ou. C.-C.; Thich, J. A.; Potenza, J. A.; Felthouse, T. R.; Haddad, M. S.; Hendrickson, D. N.; Furey, W., Jr.; Lalancette, R. A. *Inorg. Chem.* **1980**, *19*, 543.
(11) Birker, P. J. M. W. L. *Inorg. Chem.* **1979**, *18*, 3502.
(12) Groeneveld, C. M.; van Rijn, J.; Reedijk, J.; Canters, G. W. *J. Am. Chem. Soc.* **1988**, *110*, 4893.

0002-7863/90/1512-3452$02.50/0

Scheme I. Synthesis of 2,2'-Bis(2-imidazolyl)biphenyls[a]

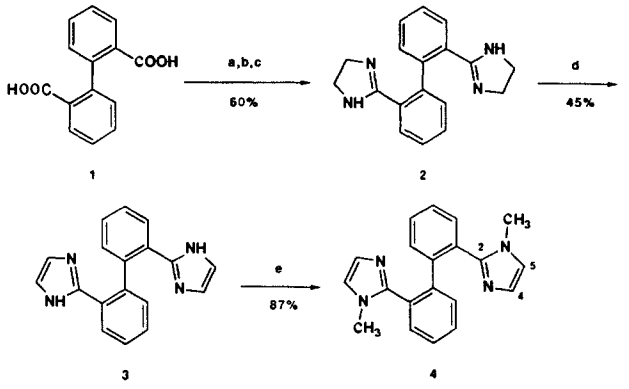

[a] Reagents and conditions: (a) $SOCl_2$, heat; (b) sulfamide, sulfolane, 180 °C; (c) ethylenediamine monotosylate, 200 °C, 10 h; (d) $BaMnO_4$, EtOAc, reflux, 16 h; (e) KH, MeI, THF, HMPA.

A distorted tetrahedral, rather than elongated C_{3v}, geometry has been inferred for Cu(II) doped into the native Zn(II) site of superoxide dismutase,[13] a cuprozinc protein that, in the native form, contains five-coordinate Cu(II) and tetrahedral Zn(II) ions bridged by an imidazolate group.[15] It is also possible to dope Ni(II) into the native Zn(II) site.[14] In the preparation of models for the tetrahedral sites in these proteins, a particularly vexing problem has been to find a way to overcome the ligand field (LF) driven distortion of tetrahedral Cu(II) and Ni(II) imidazole complexes toward planarity. Bidentate and polydentate N-donor ligands have been shown[16-21] to yield nonplanar $Cu^{II}N_4$ and $Ni^{II}N_4$ complexes with MN_2/MN_2' dihedral angles ranging up to 71.9°, but the tetrahedral limit of 90° has remained elusive.

Examination of molecular models suggested to us that a bulky, constrained bidentate ligand with a large "bite" angle might form bis complexes with first-row transition-metal ions that would be substantially distorted from planarity toward a tetrahedral coordination geometry even with metals that have a strong preference for tetragonal coordination. Such a ligand is the heretofore unknown 2,2'-bis(2-imidazolyl)biphenyl (**3** = L). We report here the synthesis of **3** and its 2:1 complexes with Cu(II) (**5**), Ni(II) (**6**), Co(II) (**7**), Cu(I) (**8**), and Zn(II), as well as the structural characterization, by single-crystal X-ray analysis, of **5–8**. We discuss the effects of ligand constraints in producing distorted tetrahedral (D_{2d} flattened) $MN(imH)_4$ coordination spheres for the various metal ions and the effects that such distortion has on the observed LF spectra and imH → M(II) charge-transfer spectra. In plastocyanin, absorptions in the near-UV region have been assigned as imH → Cu(II) charge transfer on the basis of their polarizations.[22] On the basis of studies of tetragonal Cu(II)–imidazole models, pseudotetrahedral Cu(II)–pyrazole models, and the electronic-structural relationships of these ligands, we had previously predicted that pseudotetrahedral Cu(II)–imidazole chromophores would exhibit charge-transfer absorptions in the near-UV region.[23] However, it is still desirable to study imidazole → Cu(II) charge transfer in pseudotetrahedral systems directly and to determine its blue shift when Cu(II) is replaced by the less oxidizing Ni(II) and Co(II) ions. We also compare electronic spectral and X-band EPR data with those of relevant native or derivatized proteins. Finally, we use the N-methylated derivatives of **5** and **8**, Cu(II) and Cu(I) complexes with identical ligand sets and demonstrably similar coordination geometries, to examine the rate of Cu(I/II) electron self-exchange. Comparison is made with electron self-exchange rates reported for the blue copper proteins[12] and various inorganic Cu(I)/Cu(II) redox couples.[12,24-26]

Experimental Section

1. Preparation of the Ligands. Apparatus and Reagents. Melting points were determined with an Electrothermal apparatus and are uncorrected. Infrared spectra were recorded by using a Mattson Cygnus 100 FT-IR spectrophotometer; absorption maxima are in reciprocal centimeters. Proton and carbon NMR spectra were obtained with a Varian XL-400 spectrometer. Chemical shifts are reported in parts per million downfield from tetramethylsilane (TMS) with either TMS or the solvent signal as an internal reference. Coupling constants are in hertz. Elemental analyses were performed by Galbraith Laboratories, Inc., Knoxville, TN, and Robertson Labs, Madison, NJ. Chemical ionization mass spectra (CI-MS) were obtained by use of a VG Analytical Model 7070 EQ spectrometer with isobutane as the ionizing gas. Solvents used for the synthetic work were reagent grade and were used as received except for pentane, hexamethylphosphoramide, dichloromethane, and triethylamine, which were distilled from calcium hydride, and tetrahydrofuran (THF), which was distilled from lithium aluminum hydride. Machery Nagel silica gel 60 (230–400 mesh) was employed for column chromatography.

2,2'-Biphenyldicarbonitrile. A mixture of 24.2 g (86.7 mmol) of dichlorodiphenate[27] and 25.0 g (258 mmol) of sulfamide was dissolved in sulfolane (80 mL) and heated at 180 °C for 3 h.[28] The reaction was allowed to cool and the mixture was poured into 650 mL of 1 M aqueous sodium hydroxide with stirring. The resulting precipitate was filtered and washed with water (2 × 100 mL). The solids were air-dried and crystallized from ethyl acetate to give 16.24 g (92% yield) of beige solid: mp 167–170 °C (lit.[29] mp 173–174 °C): CI-MS 205 $(M + 1)^+$.

2,2'-Bis(2-imidazolinyl)biphenyl (2). A mixture of 14.5 g (71 mmol) of the dinitrile and 133 g (568 mmol) of (2-aminoethyl)ammonium *p*-toluenesulfonate[30] was heated at 200 °C with vigorous stirring under a slow stream of nitrogen (to prevent sublimation of the dinitrile) for 10 h. As the mixture cooled, the reaction flask was rotated slowly so that solids would form over a large surface area. The reaction mixture was allowed to cool and 250 mL of 15% aqueous sodium hydroxide was added, releasing a flocculent, white precipitate. The white solid was filtered and washed consecutively with 15% aqueous sodium hydroxide (2 × 100 mL), water (100 mL), and acetone (100 mL) to give 16.8 g (82% yield) of a beige solid: mp 213–214 °C; ^1H NMR (deuteriochloroform) 3.45–3.53 (m, 4 H), 7.18 (dd, 1 H, J = 5.5, 2), 7.39–7.41 (m, 2 H), 7.71 (dd, 1 H, J = 7, 2.5); CI-MS 291 $(M + 1)^+$; IR (film) 3122, 2925, 2857, 1600, 1512, 1273, 984, 777. Anal. Calcd for $C_{18}H_{18}N_4$: C, 74.47; H, 6.25; N, 19.30. Found: C, 74.25; H, 6.31; N, 19.09.

2,2'-Bis(imidazolyl)biphenyl (3 = L). A mixture of 2.8 g (9.6 mmol) of **2**, 39.3 g (154 mmol) of freshly prepared barium manganate,[31-34] and

(13) Pantoliano, M. W.; Valentine, J. S.; Nafie, L. A. *J. Am. Chem. Soc.* **1982**, *104*, 6310.
(14) Ming, L.-J.; Valentine, J. S. *J. Am. Chem. Soc.* **1987**, *109*, 4426.
(15) (a) Richardson, J. E.; Thomas, K. A.; Rubin, B. H.; Richardson, D. C. *Proc. Natl. Acad. Sci. U.S.A.* **1975**, *72*, 1349. (b) Tainer, J. A.; Getzoff, E. D.; Beem, K. M.; Richardson, J. S.; Richardson, D. C. *J. Mol. Biol.* **1982**, *160*, 181.
(16) Johnson, J. E.; Beineke, T. A.; Jacobson, R. A. *J. Chem. Soc. A* **1971**, 1371.
(17) Baxter, C. E.; Rodig, O. R.; Schlatzer, R. K.; Sinn, E. *Inorg. Chem.* **1979**, *18*, 1918.
(18) Gouge, E. M.; Geldard, J. F. *Inorg. Chem.* **1978**, *17*, 270.
(19) Patmore, D. J.; Rendle, D. F.; Storr, A.; Trotter, J. *J. Chem. Soc., Dalton Trans.* **1975**, 718.
(20) Davis, W. M.; Zask, A.; Nakanishi, K.; Lippard, S. J. *Inorg. Chem.* **1985**, *24*, 3737.
(21) Davis, W. M.; Roberts, M. M.; Zask, A.; Nakanishi, K.; Nozoe, T.; Lippard, S. J. *J. Am. Chem. Soc.* **1985**, *107*, 3864.
(22) Penfield, K. W.; Gay, R. R.; Himmelwright, R. S.; Eickman, N. C.; Norris, V. A.; Freeman, H. C.; Solomon, E. I. *J. Am. Chem. Soc.* **1981**, *103*, 4382.
(23) Bernarducci, E.; Schwindinger, W. F.; Hughey, J. L., IV; Krogh-Jespersen, K.; Schugar, H. J. *J. Am. Chem. Soc.* **1981**, *103*, 1686.
(24) Pulliam, E. J.; McMillan, D. R. *Inorg. Chem.* **1984**, *23*, 1172.
(25) Goodwin, J. A.; Wilson, L. J.; Stanbury, D. M.; Scott, R. A. *Inorg. Chem.* **1989**, *28*, 42.
(26) Goodwin, J. A.; Stanbury, D. M.; Wilson, L. J.; Eigenbrot, C. W.; Scheidt, W. R. *J. Am. Chem. Soc.* **1987**, *109*, 2979.
(27) Bell, F.; Robinson, P. H. *J. Chem. Soc.* **1927**, 1695.
(28) Hulkenberg, A.; Troost, J. J. *Tetrahedron Lett.* **1982**, *23*, 1505.
(29) Clough, L. A.; Underwood, H. W., Jr. *J. Am. Chem. Soc.* **1929**, *51*, 583.
(30) Oxley, P.; Short, W. F. *J. Chem. Soc.* **1947**, 497.
(31) Hughey, J. L., IV; Knapp, S.; Schugar, H. J. *Synthesis* **1980**, 489.
(32) Optimum yields were obtained when the barium manganate was prepared (ref 34) with the following changes: (a) the aqueous barium manganate solution was not heated, (b) a medium sintered glass filter was used for filtration, (c) the barium manganate was washed twice with 500 mL of water, and (d) the barium manganate was kept in a vacuum oven at 110 °C for 24 h and then in a desiccator for another 24 h. The barium manganate must then be used immediately for optimal yields.

300 mL of ethyl acetate was heated at reflux for 20 h, filtered while hot, cooled, and concentrated to dryness. Flash chromatography[35] of the residue on silica gel using 1:20 concentrated ammonium hydroxide/ethyl acetate as eluant gave 1.24 g (45% yield) of a white, crystalline solid: mp 273–274 °C; ^{1}H NMR (DMSO-d_6) 6.85 (dd, 1 H, J = 7, 3), 6.87 (br s, 2 H), 7.23 (app dt, 1 H, J = 7, 3), 7.28 (app dt, 1 H, J = 7, 3), 7.56 (dd, 1 H, J = 7, 3); ^{13}C NMR (100 MHz, methanol-d_4) 123.2 (br, s), 128.3, 129.6, 131.0, 131.7, 131.9, 141.4, 147.7; CI-MS 287, $(M + 1)^+$; IR (KBr) 1559, 1427, 1103, 941, 725.

2,2′-Bis[2-(1-methyl)imidazolyl]biphenyl (4 = Me_2L). A 400-mg (3.49-mmol) mineral oil slurry of 35% potassium hydride was triturated with dry pentane (3 × 10 mL) under an argon atmosphere. A suspension of 250 mg (0.87 mmol) of **3** in 152 μL (0.87 mmol) of hexamethylphosphoramide and 40 mL of THF was added. The resulting mixture was stirred vigorously for 1 h, and then 216 μL (3.49 mmol) of iodomethane was added. This mixture was stirred for 1 h, quenched at 0 °C with methanol, and concentrated under reduced pressure. The residue was dissolved in diethyl ether (100 mL), filtered, concentrated at reduced pressure, and chromatographed on silica gel with ethyl acetate as the eluant to give 240 mg (87% yield) of **4**: mp 142–143 °C; ^{1}H NMR (deuteriochloroform) 3.29 (s, 3 H), 6.78 (s, 1 H), 6.93 (s, 1 H), 7.01 (d, 1 H, J = 7), 7.29–7.33 (m, 2 H), 7.41 (d, 1 H, J = 7); ^{13}C NMR (50 MHz, methanol-d_4) 34.4, 122.8, 128.3, 128.5, 130.3, 132.2, 132.6, 142.3, 147.9; CI-MS 315, $(M + 1)^+$; IR (film) 3106, 3060, 2948, 1464, 1280, 916, 726. Anal. Calcd for $C_{20}H_{18}N_4$: C, 76.41; H, 5.77; N, 17.82. Found: C, 76.13; H, 5.61; N, 17.59.

2. Preparation of the Complexes (L = 3). Bis[2,2′-bis(2-imidazolyl)biphenyl]copper(II) Diperchlorate, $Cu^{II}L_2(ClO_4)_2$ (5). A solution of 50 mg (0.174 mmol) of **3** in 3 mL of methanol was treated with 32 mg (0.086 mmol) of copper(II) perchlorate hexahydrate. The resulting green solution was concentrated at reduced pressure and dissolved in 3 mL of acetone. Slow vapor diffusion of diethyl ether at room temperature gave 53 mg (76% yield) of elongated prisms that exhibited yellow-green dichroism when viewed in polarized light.

$M^{II}L_2(ClO_4)_2$·3EtOH, M = Ni, (6); Co, (7); Zn. These complexes were prepared in a manner analogous to the copper(II) salt **5**. Crystals were obtained by slow vapor diffusion of diethyl ether at room temperature into ethanol solutions of the complexes. The Ni(II) complex **6** crystallized as rectangular-based prisms that exhibited green/green-orange dichroism in polarized light. The Co(II) complex **7** crystallized as rectangular-based prisms that exhibited blue-purple/red-purple dichroism. Formula weights for **6** and **7**, calculated from unit cell and density measurements, were consistent with three ethanol solvate molecules per metal ion, and this was confirmed by X-ray analysis (see below). The corrected magnetic moments of **6** and **7** at 298 K are 3.7 and 4.7 μ_B, respectively.

Bis[2,2′-bis(2-imidazolyl)biphenyl]copper(I) Perchlorate, $Cu^IL_2(ClO_4)$ (8). A solution of 15 mg (0.052 mmol) of **3** in 2 mL of dry, deoxygenated acetonitrile was treated with 8 mg (0.026 mmol) of $[Cu^I(CH_3CN)_4]ClO_4$[36] and a small amount of copper wire. Slow vapor diffusion of diethyl ether at room temperature gave brick-shaped crystals after 1 week. The crystals exhibited pale-yellow/dark-yellow dichroism.

Bis[2,2′-bis[2-(1,1-dimethyl)imidazolyl]biphenyl]copper(II) Bis(tetrafluoroborate), $Cu^{II}(Me_2L)_2(BF_4)_2$, (9). This complex was prepared in the same manner as **5**.

3. Magnetic Measurements. Acetonitrile-d_3, chloroform-d, and methanol-d_4 were obtained from Aldrich (99% isotopic purity) and were used as received. Samples for the T_1 and T^*_2 measurements were prepared in a nitrogen-filled drybox by the addition of a stock solution of $[Cu^I(CH_3CN)_4]BF_4$[36] to a solution of the ligand in acetonitrile-d_3, which had been deoxygenated by repeated freeze–pump–thaw cycles. The copper(II) complex, $Cu^{II}(Me_2L)_2(BF_4)_2$, was added to the appropriate solution in the drybox. ^{1}H data were obtained at temperatures between −30 and +50 °C with the Varian XL-400 spectrometer using 5-mm Teflon-silicone septum screw-cap NMR sample tubes (Wilmad). Typically, 32 pulses (30° tilt angle, 1-s acquisition time, 20-s delay) gave suitable spectra. Chemical shifts are referenced to acetonitrile-d_2 (1.93 ppm, present as an impurity in the deuterated solvent) as an internal reference. Spin–lattice relaxation measurements were obtained by the inversion recovery method. Peak heights obtained from the spectra were used as input for a three-parameter nonlinear least-squares fit to a single exponential to obtain the T_1 value. We estimate the precision of T_1 values to be ±3–5%.

X-band EPR spectra at room temperature and at 80 K were measured with a Varian E-12 spectrometer calibrated with a Hewlett-Packard Model 5245-L frequency counter and a DPPH crystal (g = 2.0036). Analog EPR signals were electronically multiplied by 10, digitized with a 12-bit IBM A/D converter, and stored for processing by use of a 386-type PC fitted with a 16-MHz floating point math coprocessor and 3 megabytes of memory. Instructions for carrying out these procedures, along with the software for data acquisition, manipulation, and plotting either on the PC monitor, spectrometer recorder, or Hewlett-Packard digital plotter, were obtained from Dr. Philip D. Morse II, Department of Chemistry, Illinois State University, Normal, IL 61761. Further details of these procedures have been published by Dr. Morse; see *Biophys. J.* **1987**, *51*, 440a. EPR parameters were obtained with the spectra simulation program QPOWA developed in Prof. R. L. Belford's group at the Illinois ESR Research Center, 506 S. Mathews St., Urbana, IL 61801. Further details may be found in the Ph.D. theses of M. J. Nigles (1979) and A. M. Maurice (1980). The QPOWA output files from the simulations were modified locally to match the format of the data acquisition files. Calculated and observed data were displayed together and compared on the PC color monitor. Iterative simulations were continued until the simulated and observed spectra became essentially superimposible. Parameter space was then further explored to test the uniqueness of the EPR parameter set.

Magnetic susceptibility measurements were made at 298 (1) K by using the Faraday technique. Diamagnetic corrections were calculated from Pascal's constants and applied to the susceptibilities.

4. Electronic Spectra and Electrochemistry. Electronic spectra were recorded with a computer-interfaced spectrometer constructed by Aviv Associates around the monochromator of a Cary Model 14 spectrometer.

A Princeton Applied Research (PAR) Model 173 potentiostat/galvanostat coupled with a Model 175 current follower and a Model 175 universal programmer were used for the cyclic voltammetry measurements. Voltammograms were recorded on a Houston Instruments Model 2000 X–Y recorder. Experiments were performed at 23 (1) °C in acetonitrile containing 0.1 M tetraethylammonium tetrafluoroborate as the supporting electrolyte. Scan rates ranged from 50 to 500 mV s^{-1}. A PAR electrochemistry cell with a three-electrode configuration consisting of a platinum button working electrode, an SSCE reference electrode, and a platinum wire auxiliary electrode was used. The ferrocene/ferrocenium couple was used as a reference.[37,38] No corrections were made for liquid junction potentials. Solutions were deoxygenated by bubbling argon through them for several minutes prior to use, and voltammograms were recorded with the solutions under an argon atmosphere.

5. X-ray Diffraction Studies. All diffraction measurements were made on an Enraf-Nonius CAD-4 diffractometer with graphite-monochromated Mo Kα radiation. The Enraf-Nonius Structure Determination Package[39] was used for data collection, processing, and structure solution. Selected crystal and refinement data for the four crystals studied are shown in Table I. Additional details are given as supplementary material.[40] For each crystal, intensity data were corrected for decay, absorption (empirical, Ψ scan), and Lp effects. The structures were solved by direct methods[41] and refined on F by using full-matrix least-squares techniques. H atom positions were calculated by assuming idealized bond geometries. Temperature factors for the H atoms were set equal to $1.3B_N$, where N is the atom bonded to H. H atom parameters were not refined.

A crystal of **5**, $CuL_2(ClO_4)_2$, approximately 0.17 × 0.21 × 0.32 mm, was mounted on the end of a glass fiber. An E map based on 407 phases revealed the Cu and Cl atoms. The remaining non-hydrogen atoms were located on successive difference maps. The oxygen atoms in both perchlorate groups were disordered over two sites, one with approximately $^2/_3$ of the electron density and the other with $^1/_3$. Perchlorate O atoms were refined isotropically; all other non-hydrogen atoms were refined

(33) Further application of $BaMnO_4$ to imidazole synthesis: (a) Tolman, W. B.; Rardin, R. L.; Lippard, S. J. *J. Am. Chem. Soc.* **1989**, *111*, 4532. (b) Zimmerman, S. C.; Cramer, K. D.; Galan, A. A. *J. Org. Chem.* **1989**, *54*, 1256. (c) Traylor, T. G.; Hill, K. W.; Tian, Z.-Q.; Rheingold, A. L.; Peisach, J.; McCracken, J. *J. Am. Chem. Soc.* **1988**, *110*, 5571.

(34) Firouzabadi, H.; Ghaderi, E. *Tetrahedron Lett.* **1978**, 839.

(35) Still, W. C.; Kahn, M.; Mitra, A. *J. Org. Chem.* **1978**, *43*, 2923.

(36) The perchlorate and tetrafluoroborate salts of copper(I)tetrakis(acetonitrile) were prepared by reduction of the appropriate copper(II) hydrate salts in hot acetonitrile with 200 mesh copper powder (Aldrich). Filtration of the decolorized solution while hot, followed by crystallization and isolation of the crystalline material under a nitrogen atmosphere, afforded pure $Cu^I(CH_3CN)_4X$, X = ClO_4, BF_4. See: Knapp, S.; Trope, A. F.; Theodore, M. S.; Hirata, N.; Barchi, J. J. *J. Org. Chem.* **1984**, *49*, 608.

(37) Gagne, R. R.; Koval, C. A.; Lisensky, G. C. *Inorg. Chem.* **1980**, *19*, 2854.

(38) Gritzner, G.; Kuta, J. *Pure Appl. Chem.* **1984**, *56*, 461.

(39) Enraf-Nonius Structure Determination Package, Enraf-Nonius, Delft, Holland, 1983.

(40) Supplementary material.

(41) Main, P.; Fiske, S. J.; Hull, S. E.; Germain, G.; Declercq, J.-P.; Woolfson, M. M. MULTAN 82. A System of Computer Programs for the Automatic Solution of Crystal Structures from X-ray Diffraction Data. University of York, England and Louvain, Belgium, 1982.

Table I. Crystal and Refinement Data[a]

	5	6	7	8
formula	$Cu(C_{18}H_{14}N_4)_2(ClO_4)_2$	$Ni(C_{18}H_{14}N_4)_2(ClO_4)_2{\cdot}3C_2H_6O$	$Co(C_{18}H_{14}N_4)_2(ClO_4)_2{\cdot}3C_2H_6O$	$Cu(C_{18}H_{14}N_4)_2(ClO_4)$
fw	835.12	968.50	968.72	735.67
a, Å	17.581 (3)	26.842 (5)	27.239 (4)	20.922 (7)
b, Å	21.706 (2)	13.022 (2)	13.041 (2)	20.603 (3)
c, Å	19.154 (2)	16.406 (2)	16.205 (2)	16.127 (3)
β, deg	90	126.21 (1)	125.39 (1)	90.36 (2)
V, Å^3	7309 (3)	4627 (1)	4693 (1)	6951 (5)
space group	*Pbcn*	*C2/c*	*C2/c*	*C2/c*
Z	8	4	4	8
d_{calcd}, g/cm^3	1.52	1.39	1.37	1.41
d_{obsd}, g/cm^3	1.51 (1)	1.39 (1)	1.41 (1)	1.40 (1)
linear abs coeff, cm^{-1}	8.1	6.0	5.4	7.6
rel trans factor range	0.98–1.00	0.98–1.00	0.99–1.00	0.97–1.00
data colln method	θ–2θ	θ–2θ	θ–2θ	θ–2θ
2θ range, deg	4–45	4–45	4–45	4–40
temp, K	298 (1)	298 (1)	297 (1)	298 (1)
scan rate, deg/min	0.6 + 0.35 tan θ	0.7 + 0.30 tan θ	0.70 + 0.30 tan θ	0.70 + 0.30 tan θ
no. of std refs	3	3	3	3
% var in std intens	±0.3	±6.5	±0.8	±0.7
no. of unique data colltd	4764	2934	3144	3224
no. of obsd data	2805	2049	2019	2253
final largest shift/esd	0.80	0.32	0.65	0.09
highest pk in final diff map, e/A^3	0.62	0.67	0.50	0.70
final goodness of fit	2.50	2.25	2.44	1.94
final R_F	0.077	0.080	0.061	0.070
final R_{wF}	0.088	0.085	0.076	0.071

[a] Weights were assigned as $w = 4(F_o)^2/(\sigma(F_o)^2)^2$ where $\sigma(F_o)^2 = [S^2(c + R^2B) + (PF_o^2)^2]/(Lp)^2$, S is the scan rate, C is the integrated peak count, R is the total background count, and P is a factor used to downweight intense reflections. For these structures, $P = 0.04$.

anisotropically. Refinement converged with R_F and R_{wF} equal to 0.077 and 0.088, respectively. The largest peak on the final difference map, 0.62 e/Å^3, was located 1.09 Å from Cu(1).

A crystal of **6**, $NiL_2(ClO_4)_2{\cdot}3C_2H_5OH$, 0.32 × 0.32 × 0.15 mm, was mounted inside a glass capillary that contained a small amount of mother liquor well removed from the crystal. The unit cell parameters suggested that the Ni(II) and Co(II) complexes are isostructural, and the structure was solved in the same way as the Co(II) structure (see below). In the centrosymmetric space group $C2/c$, an E map based on 306 phases revealed the Ni and several ligand atoms. The remaining non-hydrogen atoms were located on successive difference maps. The cation was found to have C_2 crystallographic symmetry. One lattice ethanol was located on a general position and the second was situated on a site of 2-fold symmetry. The diad axis is coincident with the C–O atoms in ethanol; the methyl group is removed from this axis and shows a 2-fold positional disorder. All non-hydrogen atoms were refined anisotropically. Refinement proceeded smoothly and led to convergence with R_F and R_{wF} equal to 0.080 and 0.085, respectively. Thermal parameters for the perchlorate ion and the ethanol solvate atoms were significantly higher than those of the cation, indicating that they are held loosely in the lattice. The largest peak on a difference map, 0.67 e/Å^3, was located 1.87 Å from Cl(1).

A crystal of **7**, $CoL_2(ClO_4)_2{\cdot}3C_2H_5OH$, 0.20 × 0.32 × 0.46 mm, was mounted inside a glass capillary along with a small amount of mother liquor. Diffractometer examination of the reciprocal lattice revealed systematic absences consistent with the monoclinic space groups Cc and $C2/c$. Attempted refinement in Cc gave negative temperature factors and large residuals. The structure was solved successfully in $C2/c$. An E map based on 306 phases revealed the Co atom and several ligand atoms. The remaining non-hydrogen atoms were located on successive difference maps. In contrast to the Ni structure **6**, both the perchlorate oxygen atoms and the ethanol situated in a general position exhibited positional disorder. Based on electron densities, both disorders were treated by assuming two sites with an 80/20% distribution for perchlorate atoms and a 90/10% distribution for the ethanol atoms. Parameters for the minor site atoms were not refined; all other atoms were refined anisotropically. Refinement proceeded smoothly and led to convergence with R_F and R_{wF} equal to 0.061 and 0.076, respectively. The largest peak on a final difference map, 0.50 e/Å^3, was located 2.12 Å from the Cl atom and 1.32 Å from the disordered $O(ClO_4)$ atom O(2P).

A crystal of **8**, $CuL_2(ClO_4)$, approximately 0.25 × 0.15 × 0.15 mm, was glued inside a glass capillary and sealed under argon. Systematic absences were consistent with space groups Cc or $C2/c$. The structure was solved and successfully refined in the centrosymmetric space group $C2/c$. An E map based on 385 phases revealed the Cu and several ligand atoms. The remaining non-hydrogen atoms were located readily from successive difference maps. The perchlorate oxygen atoms were disordered over two sites in an approximate 80/20% ratio. Major site parameters were refined isotropically; minor site parameters were not refined. Refinement led to convergence with R_F and R_{wF} equal to 0.070 and 0.071, respectively. The largest 11 peaks on a final difference map,

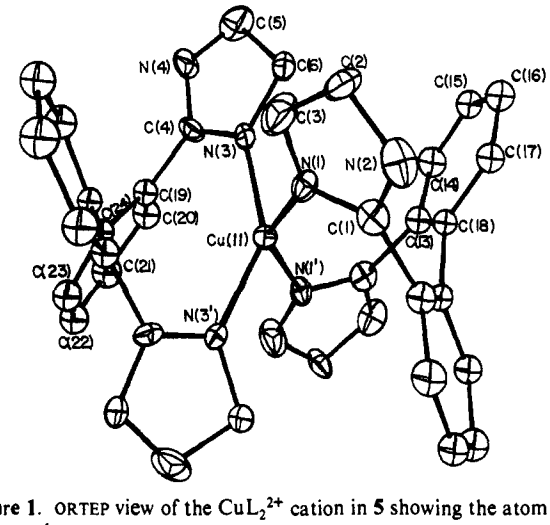

Figure 1. ORTEP view of the CuL_2^{2+} cation in **5** showing the atom numbering scheme.

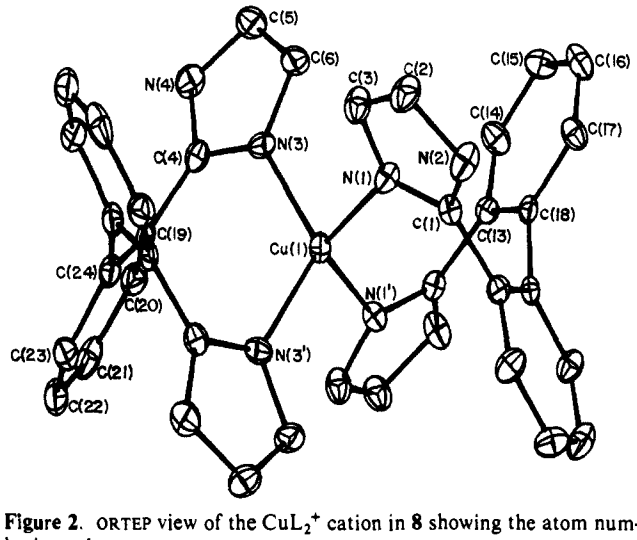

Figure 2. ORTEP view of the CuL_2^+ cation in **8** showing the atom numbering scheme.

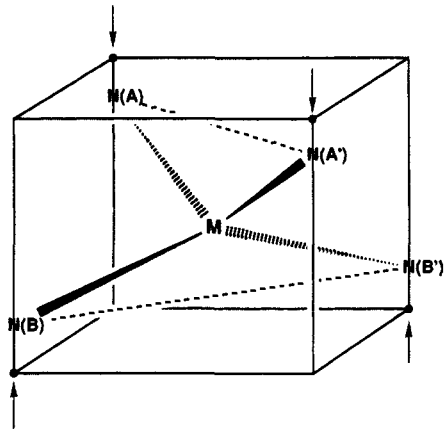

Figure 3. Sketch showing an idealized D_{2d} MN_4 coordination geometry for the ML_2 species. The four marked corners of the cube indicate ligand atom locations for tetrahedral geometry; the arrows indicate the direction of motion required to produce D_{2d} symmetry.

0.43–0.70 $e/Å^3$, were located 1.40–1.65 Å from the Cl atom.

Views of the cations for the Cu^{I} and Cu^{II} complexes are shown in Figures 1 and 2, respectively. Lists of atomic coordinates, isotropic and anisotropic thermal parameters, bond distances and angles, and observed and calculated structure factors are available.[40]

Results and Discussion[42]

1. Ligand Synthesis. The ligand **3** was prepared from commercially available diphenic acid (**1**, Scheme I) via the bis(imidazoline) **2**. Treatment of the carboxylic acid chloride[27] derived from **1** with sulfamide[28] gave an intermediate aroylsulfonamide, which eliminated sulfamic acid at elevated temperature, producing the known[29] 2,2′-biphenyl bis(carbonitrile). Condensation of the bis(nitrile) with the mono(tosylate) salt of ethylenediamine under standard conditions[30] gave the bis(imidazoline) **2**, and oxidation[31-33] of **2** using barium manganate[34] followed by chromatography afforded the bis(imidazole) ligand **3**. Gram quantities of pure **3** could thus be prepared in ~27% overall yield from diphenic acid. The N,N-dimethylated derivative **4**, which was used for the NMR relaxation studies, was prepared by treatment of **3** with potassium hydride and iodomethane.

2. Crystal Structures. Each of the structures **5–8** contains ML_2^{n+} cations [M = Cu(II), **5**; Ni(II), **6**; Co(II), **7**; and Cu(I), **8**] separated by perchlorate anions and, for **6** and **7**, lattice ethanol molecules as well. All the metal ions are situated on special positions with C_2 site symmetry. For complexes **5** and **8**, there are two unique Cu atoms in each structure. This gives rise to two crystallographically distinct molecules in the unit cell, each with C_2 point symmetry. In **5**, the diad axes pass through the centers of the biphenyl bridges of the two ligands for both cations (see **10**). In **8**, the two unique cations are oriented differently. In one cation, the 2-fold axis bisects the ligands as in **10**, while in the other, it produces one ligand from the other as in **11**. For the Ni(II) and Co(II) structures, the diad axes are as in **11**. In all four complexes, individual cations are chiral owing to the helical biaryl substructure, and because the space groups contain symmetry elements of reflection, all of the crystals are racemates.

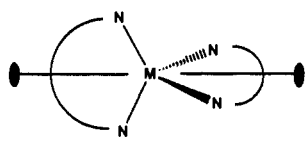

10

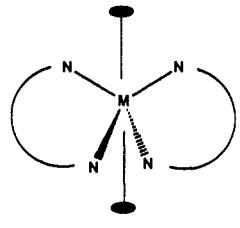

11

(42) A preliminary version of this work in which some of these results are described has appeared: Knapp, S.; Keenan, T. P.; Zhang, X.; Fikar, R.; Potenza, J. A.; Schugar, H. J. *J. Am. Chem. Soc.* **1987**, *109*, 1882.

Table II. Selected Bond Distances (Å) and Angles (deg) for **5–8**

	5	6	7	8
metal, M	Cu(II)	Ni(II)	Co(II)	Cu(I)
Bond Distances in Coordination Sphere				
M–N(1)[a]	1.950 (8)	1.960 (4)	1.987 (3)	2.029 (6)
	1.977 (8)			2.031 (6)
M–N(3)	1.962 (8)	1.966 (4)	2.002 (3)	2.035 (6)
	1.941 (9)			2.053 (6)
M–N–C Angles				
M–N–C(D), γ[b]	120.8 (8)	123.6 (3)	126.2 (3)	125.8 (6)
	120.7 (8)	122.6 (4)	125.2 (3)	125.3 (7)
	120.5 (8)			125.3 (6)
	121.5 (9)			126.7 (6)
M–N–C(E), δ	135.7 (9)	126.8 (4)	123.8 (3)	123.8 (6)
	131.5 (8)	129.6 (4)	125.7 (3)	124.5 (6)
	134.5 (9)			127.7 (6)
	131.5 (9)			122.5 (6)
Nine-Membered Chelate Ring Angles, α				
N(1)–M–N(3)[c]		130.2 (2)	123.2 (1)	120.6 (3)
N(1)–M–N(1′)	140.9 (5)			119.7 (4)
	142.1 (5)			
N(3)–M–N(3′)	143.2 (5)			121.6 (4)
	141.4 (5)			
Interligand Angles, β				
N(1)–M–N(3′)		98.1 (2)	102.5 (1)	104.4 (3)
N(1)–M–N(1′)		100.1 (2)	101.6 (2)	107.3 (3)
N(3)–M–N(3′)		104.6 (2)	105.5 (2)	100.6 (4)
N(1)–M–N(3)	92.7 (3)			105.7 (2)
	93.7 (4)			
N(1)–M–N(3′)	99.4 (3)			102.7 (3)
	98.7 (3)			
Dihedral Angles				
N(A)–M–N(A′)[c]	86.3 (2)	87.6 (2)	89.5 (1)	88.0 (2)
intraligand	87.2 (2)			89.5 (2)
N(A)–M–N(B)	53.4 (3)	65.4 (2)	74.4 (1)	76.8 (2)
interligand	50.5 (3)	67.7 (2)	75.0 (1)	77.9 (2)
	53.5 (3)			78.7 (2)
	51.2 (3)			77.5 (2)
imH/phenyl	63.3 (5)	51.3 (3)	52.2 (2)	53.6 (4)
	63.5 (5)	56.0 (3)	57.1 (2)	68.4 (3)
	61.6 (6)			54.5 (4)
	58.3 (6)			53.3 (4)
average	61.7	53.7	54.7	57.5
phenyl/phenyl	54.1 (3)	63.6 (3)	65.7 (2)	68.8 (2)
	58.8 (3)			65.1 (3)
	55.9 (3)			65.0 (2)
	59.2 (3)			
average	57.0	63.6	65.7	66.3
Bay Contacts				
C(A)···C(B)[b]	3.19 (2)	3.204 (9)	3.241 (7)	3.30 (1)
	2.97 (2)	3.28 (1)	3.300 (9)	3.26 (1)
	3.13 (2)			3.22 (1)
	3.03 (2)			3.24 (1)
average	3.08	3.24	3.27	3.26
N···C(C)[b]	3.24 (2)	3.10 (1)	3.07 (1)	3.09 (1)
	3.15 (2)	3.125 (9)	3.119 (8)	3.09 (1)
	3.25 (2)			3.08 (1)
	3.18 (2)			
average	3.21	3.11	3.09	3.09

[a] Numbered atoms numbers refer to the coordinates listed in the supplementary material and depicted in Figures 1 and 2 for **5** and **8**, respectively. [b] Atoms C(A)–C(E) are defined in the text (see **12**). [c] Lettered nitrogen atoms refer to the type shown in Figure 3.

The geometry of the coordination spheres is distorted from tetrahedral, with varying amounts of D_{2d} flattening. The degree of D_{2d} flattening in the four structures can be gauged by the data in Table II. The dihedral angle between ligands N(A)–M–N(A′)/N(B)–M–N(B′) for all four structures is within 4° of the ideal tetrahedral value (90°, Figure 3). Deviations from T_d symmetry are most clearly evident in the intraligand angles N(A)–M–N(A′) (Figure 3). These increase from approximately 120° in the Cu(I) structure **5** to 140° in the Cu(II) structure **8**. Thus, D_{2d} flattening is greatest in the Cu(II) complex followed

Table III. Values of θ and Average Values of α and β for **5–8**

	α_{obs}(av)	β_{obs}(av)	β_{calcd}	θ_x	θ_y	θ_z
Cu(II), **5**	141.6 (9)	96.2 (34)	96.2	90.0	90.0	86.3 (2)
				90.0	90.0	87.2 (2)
Ni(II), **6**	130.2 (2)	101.0 (30)	100.2	87.0	87.1	87.6 (2)
Co(II), **7**	123.2 (2)	103.2 (22)	103.1	87.5	87.6	89.5 (1)
Cu(I), **8**	120.6 (10)	104.1 (28)	104.2	90.0	90.0	88.0 (2)
				86.0	86.0	89.5 (2)

by the Ni(II), Co(II), and Cu(I) complexes. Two factors appear to be responsible for the D_{2d} flattening: (1) geometric constraints within the nine-membered chelate rings cause the intraligand angles to exceed the tetrahedral value, flattening the otherwise tetrahedral CuN_4 units, and (2) additional ligand field effects result in larger angles for the Cu(II) and Ni(II) complexes compared with those of Co(II) and Cu(I), species that typically form tetrahedral complexes. Finally, we note that increasing D_{2d} flattening is also reflected by the successive decrease in the interligand dihedral angles N(A)–M–N(B')/N(B)–M–N(A'), which vary from ca. 78° in the Cu(I) structure to ca. 53° in the Cu(II) cations.

In the four structures, the coordination spheres of the individual cations deviate only slightly from D_{2d} symmetry. In point group D_{2d}, the intraligand angles [N(A)–M–N(A'), α] are related to the four simple interligand angles [N(A)–M–N(B), β] by eq 1.[43]

$$\beta = \cos^{-1}[-\cos^2(\alpha/2)] \quad (1)$$

Average observed values of α and β are shown in Table III, along with calculated values of β. For all structures, the observed and calculated values agree within experimental error. A second measure of the deviation of the coordination spheres from D_{2d} symmetry is given by the three angles θ_x, θ_y, and θ_z,[43] which, for D_{2d} symmetry, are all equal to 90°. Here, θ_z is the intraligand dihedral angle (Table II) and represents a twisting of one ligand with respect to the other; deviations of θ_x and θ_y from the ideal value represent "rocking" or "wagging" displacements of ligand 2 with respect to ligand 1. Values of θ for the various cations (Table III) show that they all approximate D_{2d} symmetry to within a few degrees. For cations with the C_2 axis situated as in **10**, θ_x and θ_y are required by symmetry to be 90° and the only angular deviation from D_{2d} symmetry in these species results from twisting.

M–N bond lengths are shown in Table II. The Cu(II)–N distances are ca. 0.05 Å shorter than those generally observed for planar or tetragonal tetrakis(imidazole)copper(II) complexes[44,45] but are typical for tetrahedrally distorted Cu(II) complexes having four sp^2 N donors.[16,19,46] The Ni(II)–N distances are similar to those in pseudotetrahedral Ni(II) tropocoronand complexes with interligand dihedral angles in the range 70.1–85.2°,[21] but are ca. 0.07 Å longer than those in diamagnetic, tetragonal Ni(II) analogues. In the tetragonal case, the $d_{x^2-y^2}$ orbital is vacant, allowing close approach of the ligands along the x and y axes. In octahedral Ni(II) complexes, Ni(II)–N distances lie in the range 2.07–2.13 Å[47-49] and are longer than those in corresponding tetragonal or tetrahedral complexes. Octahedral Ni(II) complexes have high-spin magnetic properties and no p_π–d_π bonding, favoring long distances.

The Co(II)–N distances are equivalent, within experimental error, to those [1.988 (3), 2.002 (3) Å] observed for the essentially tetrahedral $(1,2\text{-dimethylimidazole})_4Co^{II}(ClO_4)_2$ complex.[50] Linear,[51] trigonal,[52] and tetrahedral[53] copper(I) complexes with imidazole or substituted imidazole ligands are known. The Cu(I)–N(imH) distances in **8** are typically 0.1–0.2 Å longer than those in the two- and three-coordinate structures and are closer to the value of 2.072 (14) Å reported for a distorted tetrahedral (dicyanoimidazole)copper(I) complex.[53] The Cu(I)–N distances in **8** are also ca. 0.07 Å longer than those in the Cu(II) complex **5**, consistent with the d vacancy and higher charge in **5**, both factors allowing closer approach of the ligands.

The ligand has three torsional degrees of freedom represented by the phenyl/phenyl and imidazole/phenyl dihedral angles (Table II). The phenyl/phenyl angles decrease with increasing D_{2d} flattening and are smallest for the Cu(II) structure **5**; just the reverse is observed for the imidazole/phenyl dihedral angles. Bay contacts of the type shown in **12** also vary systematically with the

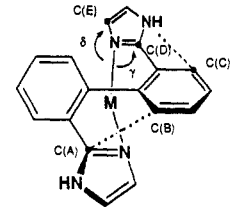

12

degree of D_{2d} flattening (Table II): as the MN_4 units distort toward a planar D_{4h} geometry, the C(A)···C(B) contacts decrease and the N···C(C) contacts increase. At the one extreme (complex **5**), atoms C(A) and C(B) appear to be in close contact, suggesting that the C(A)···C(B) distance cannot be further decreased without a substantial increase in energy. At the other extreme (complex **8**), the N···C(C) contacts are slightly smaller than the sum of the C and N van der Waals radii (ca. 3.2 Å), indicating that further decreases in the imidazole/phenyl dihedral angles cannot occur easily, regardless of the bonding requirements of the metal.

Additional insight regarding bonding of **3** to the various metals is gained by an examination of the M–N–C angles, γ and δ, defined in **12**. These angles (Table II) differ by ~14° on average for the Cu(II) complex **5**, 5° for the Ni(II) complex **6**, and are approximately equal for both the Co(II) and Cu(I) complexes **7** and **8**. In both the Cu(II) and Ni(II) structures, the angular deviations from symmetrical imidazole bonding are in a direction consistent with movement of the nitrogen atoms toward tetragonal coordination.

3. Electron Self-Exchange Rate. A number of experiments have been devised to evaluate second-order self-exchange rate constants, k, for reactions of the type shown in eq 2. where X is

$$Cu^{*II}X + Cu^{I}X = Cu^{*I}X + Cu^{II}X \quad (2)$$

any ligand set. For these systems, rate constants have been measured directly by using EPR spectroscopy to observe scrambling of isotopically pure $^{63}Cu^{II/I}X$ and $^{65}Cu^{I/II}X$ species.[54] Rate constants have also been determined indirectly from line-broadening (T^*_2), direct T_2, or spin–lattice relaxation (T_1) measurements.[55] Values for k may be calculated by using the Marcus correlation equation[56] and data obtained from reactions involving redox couples in which there is a net free energy change. It has been suggested that the latter procedure can lead to large errors in k.[57] Rate constants from ca. 10^{-5} to 10^7 M^{-1} s^{-1} have been

(43) Dobson, J. F.; Green, B. E.; Healy, P. C.; Kennard, C. H. L.; Pakawatchai, C.; White, A. H. *Aust. J. Chem.* **1984**, *37*, 649.
(44) Bernarducci, E.; Bharadwaj, P. K.; Krogh-Jespersen, K.; Potenza, J. A.; Schugar, H. J. *J. Am. Chem. Soc.* **1983**, *105*, 3860.
(45) Sundberg, R. J.; Martin, R. B. *Chem. Rev.* **1974**, *74*, 471.
(46) Schilstra, M. J.; Birker, P. J. M. W. L.; Verschoor, G. C.; Reedijk, J. *Inorg. Chem.* **1982**, *21*, 2637.
(47) Battaglia, L. P.; Corradi, A. B.; Antolini, L.; Marcotrigiano, G.; Menabue, L.; Pellacani, G. C. *J. Am. Chem. Soc.* **1982**, *104*, 2407.
(48) Konopelski, J. P.; Reimann, C. W.; Hubbard, C. R.; Mighell, A. D.; Santoro, A. *Acta Crystallogr.* **1976**, *B32*, 2911.
(49) Finney, A. J.; Hitchman, M. A.; Raston, C. L.; Rowbottom, G. L.; White, A. H. *Aust. J. Chem.* **1981**, *34*, 2113.
(50) Bernarducci, E.; Bharadwaj, P. K.; Potenza, J. A.; Schugar, H. J. *Acta Crystallogr.* **1987**, *C43*, 1511.
(51) Sorrell, T. N.; Jameson, D. L. *J. Am. Chem. Soc.* **1983**, *105*, 6013.
(52) (a) Clegg, W.; Acott, S. R.; Garner, C. D. *J. Chem. Soc., Dalton Trans.* **1984**, 2581. (b) Sorrell, T. N.; Borovik, A. S. *J. Am. Chem. Soc.* **1987**, *109*, 4255.
(53) Rasmussen, P. G.; Rongguang, L.; Butler, W. M. *Inorg. Chim. Acta* **1986**, *118*, 7.
(54) Groeneveld, C. M.; Dahlin, S.; Reinhammar, B.; Canters, G. W. *J. Am. Chem. Soc.* **1987**, *109*, 3247.
(55) Ugurbil, K.; Mitra, S. *Proc. Natl. Acad. Sci. U.S.A.* **1985**, *82*, 2039.
(56) (a) Marcus, R. A. *J. Phys. Chem.* **1963**, *67*, 853. (b) Marcus, R. A. *J. Chem. Phys.* **1965**, *43*, 679.
(57) Koval, C. A.; Margerum, D. W. *Inorg. Chem.* **1981**, *20*, 2311.
(58) McConnell, H. M.; Weaver, H. E., Jr. *J. Chem. Phys.* **1956**, *25*, 307.

Table IV. Representative Cu(II)/Cu(I) Self-Exchange Rate Constants

ligand	k, M^{-1} s^{-1}	method	ref	solvent	temp, °C
chloride	5×10^7	^{63}Cu NMR (T_2)	58	H_2O	
azurin	6×10^5	EPR ($^{63}Cu/^{65}Cu$ scrambling)	54	H_2O	4
	1×10^6	^1H NMR (T^*_2)	59	D_2O	36
	1×10^4	^1H NMR (T_1)	55	D_2O	25
stellacyanin	1×10^5	EPR ($^{63}Cu/^{65}Cu$ scrambling)	63		
TAAB[a]	5×10^5	^1H NMR (T^*_2)	24	CD_3OD	22
2,9-dimethyl-1,10-phenanthroline	2×10^4	Marcus	60	H_2O	25
$(imidH)_2DAP$[b]	1.3×10^4	^1H NMR (T^*_2)	25	CD_3CN	25
plastocyanin	$\ll 10^4$	^1H NMR (T^*_2)	61	D_2O	50
$(py)_2DAP$[c]	1.7×10^3	^1H NMR (T^*_2)	26	CD_3CN	25
bidhp[d]	4×10^3	^1H NMR (T_1, T^*_2)	12	$(CD_3)_2SO$	28
Me_2L	$<1 \times 10^2$	^1H NMR (T_1)	e	CD_3CN	−20 to +20
1,10-phenanthroline	43	Marcus	60	H_2O	25
water	1×10^{-5}	Marcus	62	H_2O	25

[a] Tetrabenzo[*b,f,j,n*][1,5,9,13]tetraazacyclohexadecine. [b] 2,6-Bis[1-[(2-imidazol-4-ylethyl)imino]ethyl]pyridine. [c] 2,6-Bis[1-[(2-pyridin-2-ylethyl)imino]ethyl]pyridine. [d] The tetradentate N_2S_2 ligand bidhp, 1,7-bis(5-methylimidazol-4-yl)-2,6-dithiaheptane, is thought to coordinate to copper in solution via two S (thioether) and two N (imidazole) linkages. [e] This work.

Table V. ^1H NMR Chemical Shifts (δ, ppm) for Cu(I) Solutions of Me_2L in CD_3CN[a]

	free ligand[b]	1:1 complex[c] Cu(I)	2:1 complex[c] Cu(I)
CH_3	3.33	3.70	3.61
imidazole H(4)	6.77	6.73	6.84
imidazole H(5)	6.95	7.09	6.01

[a] T = −20 °C; solutions of the Cu(I) complexes were prepared from Me_2L and $Cu(CH_3CN)_4(BF_4)$. A 2:1 ligand to Cu(II) solution showed three broad resonances at 9.1, 8.0, and 6.1 ppm as well as some smaller, sharp resonances arising from the 1:1 Cu(I) species, which is present as an impurity. [b] $[Me_2L]$ = 16 mM. [c] [Cu(I)] = 7.95 mM.

reported for systems with ligands ranging in complexity from chloride to proteins (Table IV).

Large rate constants are favored by several factors, including short internuclear distances, appropriate orbital overlap (to provide an electronic pathway for the exchange), and similar coordination geometries for the reduced and oxidized species (to minimize ligand and solvent reorganization). Ligand loss or exchange adds an additional complication that can affect the observed rates.[25]

In our studies, the $N(1),N(1')$-dimethyl derivative of L (standard imidazole numbering scheme; see Scheme I), **4** = Me_2L, was used because it is more soluble than **5** in acetonitrile and because it provides an additional ^1H NMR signal for the T^*_2 and T_1 studies. Use of the *N*-methyl derivative also avoids potential complications associated with N–H proton exchange as well as equilibration of the C(4) and C(5) imidazole positions due to tautomerization. Electronic spectral data (see below) and examination of molecular models suggest that the geometries of the N-methylated and nonmethylated cations should be quite similar. Data are reported for the *N*-methyl protons, the imidazole vinylene protons, and several resonances associated with the phenyl groups.

a. Ligand Exchange. To examine the solution chemistry and to determine the extent of ligand exchange, solutions of the ligand Me_2L with various concentrations of Cu^IBF_4 and $Cu^{II}(BF_4)_2$ in deuterioacetonitrile were examined by ^1H NMR spectroscopy over the −30 to +50 °C temperature range. With Cu^IBF_4, three distinct sets of signals were seen at low temperature depending upon the concentration of Cu(I) (Table V). With Cu(I) in excess, two sets of signals were seen at temperatures below −10 °C, which we assign to the 1:2 complex $Cu^I(Me_2L)_2$ and the 1:1 complex $Cu^IMe_2LX_2$, where X corresponds to solvent. Above this temperature, coalescence of the methyl signals was observed. Addition of excess ligand also resulted in two sets of signals, which we assign to the free ligand and the 1:2 complex $Cu^I(Me_2L)_2$. As the temperature of the solution with excess ligand was raised, the methyl resonances coalesced at ca. 5–10 °C and narrowed at higher temperatures (Figure 4), indicating facile ligand exchange on the NMR time scale.

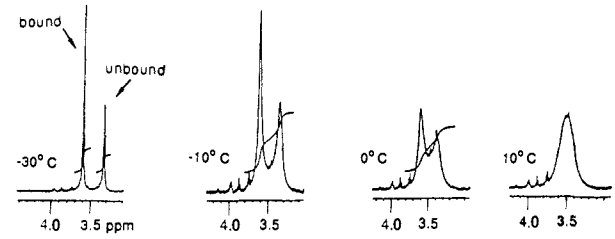

Figure 4. ^1H NMR spectra (400 MHz, CD_3CN solvent) at −30, −10, 0, and 10 °C of a solution 7.95 mM in $Cu^I(Me_2L)_2(BF_4)$ with excess Me_2L showing the coalescence of the methyl signals at ca. 5 °C. Chemical shifts at −30 °C are 3.60 and 3.33 ppm for the bound and unbound species, respectively.

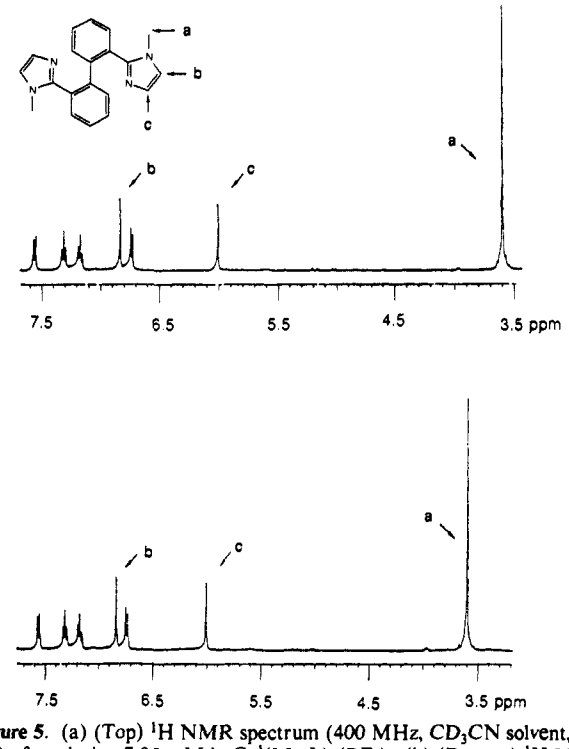

Figure 5. (a) (Top) ^1H NMR spectrum (400 MHz, CD_3CN solvent, −30 °C) of a solution 7.95 mM in $Cu^I(Me_2L)_2(BF_4)$. (b) (Bottom) ^1H NMR spectrum (400 MHz, CD_3CN solvent, −30 °C) of a solution 7.95 mM in $Cu^I(Me_2L)_2(BF_4)$ and 3.65 mM in $Cu^{II}(Me_2L)_2(BF_4)_2$.

(59) Groeneveld, C. M.; Canters, G. W. *Eur. J. Biochem.* **1985**, *153*, 559.
(60) Yandell, J. K. In *Copper Coordination Chemistry: Biochemical and Inorganic Perspectives*; Karlin, K. D., Zubieta, J., Eds.; Adenine Press: Guilderland, NY, 1983; pp 157–166.
(61) Beattie, J. K.; Fensom, D. J.; Freeman, H. C.; Woodcock, E.; Hill, H. A. O.; Stokes, A. M. *Biochim. Biophys. Acta* **1975**, *405*, 109.
(62) Hoselton, M. A.; Lin, C.-T.; Schwarz, H. A.; Sutin, N. *J. Am. Chem. Soc.* **1978**, *100*, 2383.
(63) Dahlin, S.; Reinhammar, B.; Wilson, M. T. *Inorg. Chim. Acta* **1983**, *79*, 126.

Table VI. Spin-Lattice Relaxation Times (s) at −20 °C

signal	δ, ppm	T_{10}, 0% Cu(II)[a]	T_1, 10% Cu(II)[a]	T_1, 20% Cu(II)[a]	T_1, 30% Cu(II)[a]	T_1, 40% Cu(II)[a]
methyl	3.61	0.82	0.84	0.70	0.66	0.62
imidazole H(5) doublet	6.01	2.14	1.51	1.32	1.13	0.94
imidazole H(4) doublet	6.74	1.97	1.53	1.33	1.15	0.97
triplet	6.84	2.54	1.93	1.70	1.44	1.20
triplet	7.17	1.50	1.20	1.09	0.98	0.87
doublet	7.31	1.44	1.17	1.05	0.93	0.84
	7.56	1.39	1.12	0.98	0.88	0.78

[a] All measurements were made in CD_3CN, with the concentration of $Cu^I(Me_2L)_2$ equal to 12.5 mM; concentrations of $Cu^{II}(Me_2L)_2$ were as follows: 10%, 1.25 mM; 20%, 2.50 mM; 30%, 3.75 mM; 40%, 5.00 mM.

b. Line-Broadening Studies. In an attempt to determine the electron self-exchange rate constant, known quantities of $Cu^{II}(Me_2L)_2$ (2%, 11%, and 46%) were added to solutions of $Cu^I(Me_2L)_2$ at −20 and +20 °C. Even in the most concentrated solution, separate sets of signals were observed for the Cu(I) and Cu(II) species with no appreciable line broadening of either the methyl or vinylene protons (Figure 5). Repetition of the same experiment with a solution additionally 200 mM in tetrabutylammonium bromide had no further effect on line broadening. These observations can be used to set an upper limit for k. In the slow-exchange limit,[24] eq 3 applies, where $\Delta\nu$ is the NMR peak

$$\pi(\Delta\nu_2 - \Delta\nu_1) = k[\text{Cu(II)}] \quad (3)$$

width (full width at half-height) and the subscripts 2 and 1 refer to the systems with and without the Cu(II) complex, respectively. In our systems, we estimate $\Delta\nu_2 - \Delta\nu_1$ to be less than 1 Hz, the limit for detectability of line broadening in our spectra, and with the [Cu(II)] of the order of 3 mM, the upper limit for k is approximately 10^3 M^{-1} s^{-1}.

c. T_1 Studies. Cu(I)/Cu(II) self-exchange rate constants can be determined by measuring spin-lattice relaxation times of nuclei on the Cu(I)-containing cation (reduced species) in the presence of varying amounts of the paramagnetic Cu(II)-containing complex (oxidized species).[55] In our case, T_1 values for protons on $Cu^I(Me_2L)_2$ depend on the lifetime of this species which, in turn, depends on the rate of electron exchange and the concentration of the reduced species according to eq 4,[55] where T_{10} is the

$$P = (T_1^{-1} - T_{10}^{-1}) = k[\text{Cu(II)}] \quad (4)$$

spin-lattice relaxation time of a nucleus in the Cu(I) complex, T_1 is the corresponding relaxation time in the presence of the Cu(II) complex, [Cu(II)] is the concentration of the Cu(II) complex, k is the second-order self-exchange rate constant, and P is the paramagnetic induced relaxation rate. Equation 4 is valid in the slow-exchange limit and predicts that a plot of P vs [Cu(II)] should yield a straight line with zero intercept. If the [Cu(II)] is replaced by [R•], where R• is any free radical, the self-exchange rate constant k becomes the molar radical-induced relaxation rate M.

Representative values of T_1^{-1} and T_{10}^{-1}, measured at −20 °C, are listed in Table VI. Selected values, plotted in Figure 6, demonstrate the extent to which the slow-exchange limit applies in the present case. Calculated values of k, obtained with eq 4 and shown in Table VII range from approximately 80 to 150 M^{-1} s^{-1}. These figures should be regarded as an upper limit for the self-exchange constant because much of the relaxation induced by the Cu(II) species could arise from collisions between $Cu^I(Me_2L)_2$ and $Cu^{II}(Me_2L)_2$ in which no electron exchange occurs. To test this possibility, molar radical-induced relaxation rates $P/[R^•]$ were measured with bis(diphenylene)phenylallyl (BDPA, **13**) or $Ni^{II}(Me_2L)_2(ClO_4)_2$ as the paramagnetic species added to

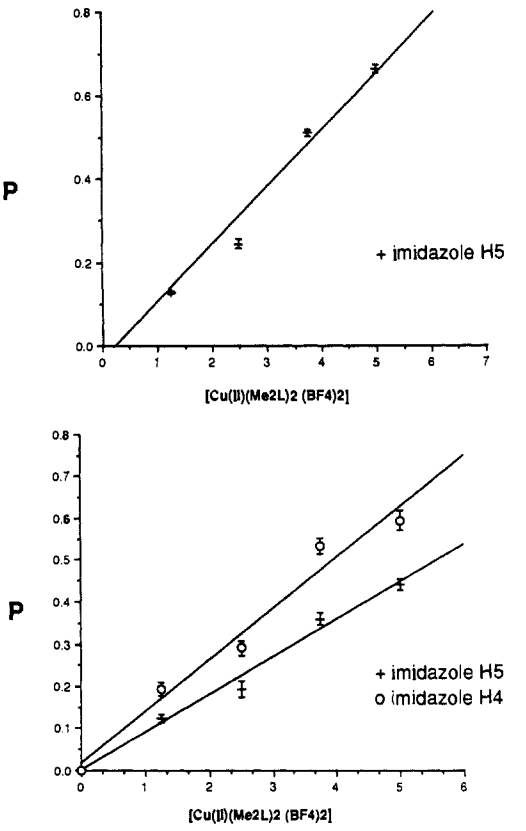

Figure 6. Plots of P vs $[Cu^{II}(Me_2L)_2(BF_4)_2]$ for (a) the imidazole H(5) NMR signal of $Cu^I(Me_2L)_2(BF_4)$ at −20 °C and (b) the imidazole H(4) and H(5) NMR signals of $Cu^I(Me_2L)_2(BF_4)$ at +20 °C. Data points were taken from Table VI.

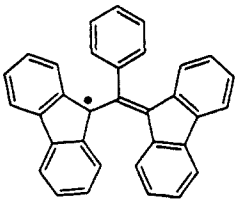

13

solutions containing $Cu^I(Me_2L)_2(ClO_4)$. As seen from the data in Table VII, rates obtained with these species are comparable to or greater than those for the copper-only systems, indicating that the bulk of the relaxation in the latter may be coming from random bounce collisions during which no electrons are exchanged. We note that the molar radical-induced relaxation rates observed with BDPA and the Ni(II) complex are not unusual. They are of the same order of magnitude (ca. 100–1000 M^{-1} s^1) as those

Table VII. Molar Radical-Induced Relaxation Rates, M (M^{-1} s^{-1})[a]

	methyl	imidazole H(5)	doublet	imidazole H(4)	triplet	triplet	doublet
δ, ppm	3.61	6.01	6.74	6.84	7.17	7.31	7.56
k/M, Cu(II) −20 °C	85	130	110	90	110	110	130
k/M, Cu(II) +20 °C	80		160	120	90	150	
M, BDPA, −20 °C	240	280	290	290	270	280	310
M, BDPA, +20 °C	410		440	420	380	420	
M, Ni(II),[b] −20 °C	80	140	60	55	40	40	40
M, Ni(II),[b] +20 °C	600	820	660	660	550	630	

[a] For a solution containing 12.5 mM $Cu^I(Me_2L)_2(BF_4)$ in CD_3CN. [b] Ni(II) = $Ni^{II}(Me_2L)_2$.

reported for neutral free radicals (of approximately the same size as the copper cations) colliding randomly with small solvent molecules at low field (75 G).[64]

The upper limit estimate for k is substantially smaller than the values reported for many of the systems listed in Table IV. In particular, it is approximately 3–4 orders of magnitude smaller than those for azurin and stellacyanin, where distances of closest approach between the redox partners are expected to be substantially longer than for the Me_2L systems and may also be smaller than the relatively small value estimated for plastocyanin. It is several orders of magnitude smaller than those for TAAB (a macrocyclic, tetramine ligand) and 2,9-dimethyl-1,10-phenanthroline, both of which might be expected to show greater differences in coordination geometry between the Cu(I) and Cu(II) complexes than Me_2L. Why is k so small? One possible explanation is that, owing to the substantial distortion of the Cu(II) coordination geometry in **5** from D_{4h} toward T_d point symmetry, the unpaired electron, which resides in the $d_{x^2-y^2}$ orbital (see EPR section below), cannot overlap effectively with the ligand orbitals (see **14**). The rate of outer-sphere electron transfer accordingly

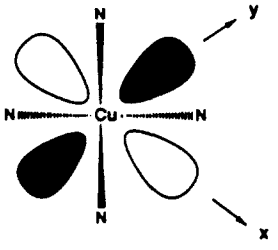

14

may be attenuated. Relatively poor electronic coupling in **5** of the Cu(II) unpaired electron with the imidazole ligation is indicated by the weakness of the imH → Cu(II) LMCT absorption, and possibly by the observability of hyperfine coupling in the EPR spectrum of the neat complex. For the blue Cu(II) site in plastocyanin, SCF-Xα calculations[65] suggest that the unpaired electron is substantially delocalized, spending only ~40% of its time in the Cu $d_{x^2-y^2}$ orbital. Delocalization of this sort could help account for the relatively large values of k for azurin and stellacyanin. Other factors, such as solvent effects, could also contribute to the small value of k.

4. EPR Studies. EPR data for **5** and related complexes are shown in Table VIII. These complexes exhibit axial spectra that are characteristic of Cu(II) complexes having $d_{x^2-y^2}$ ground states. The EPR parameters listed are those obtained by the spectral simulation procedures described in the Experimental Section. The smallest hyperfine coupling, $A_{\parallel}^{Cu} = 118 \times 10^{-4}$ cm^{-1}, and thus the closest approach to an idealized tetrahedral geometry, was observed for the polycrystalline Cu(II)-doped $Zn^{II}L_2(ClO_4)_2$ complex. Interestingly, relatively unbroadened EPR signals having resolved hyperfine coupling also could be observed for the neat Cu(II) complex **5**. The increase in hyperfine coupling from 118×10^{-4} to 130×10^{-4} cm^{-1} for the neat complex indicates that the more nearly tetrahedral structure of the Zn(II) complex is imposed on the Cu(II) dopant by lattice-packing forces. Moreover, the increase of $g_{\parallel}$ from 2.26 in the neat complex to 2.32 for the doped material also points to a more nearly tetrahedral structure for the latter.

The hyperfine coupling constant increases further to 147×10^{-4} cm^{-1} for solutions of **5** in glassed acetonitrile at 80 K. Thus, the extent of D_{2d} flattening appears to increase in the order Cu(II)-doped Zn(II) complex < neat **5** < glassed solution of **5**. The limit of D_{2d} flattening is square-planar tetrakis(imidazole) coordination. In this limit, the hyperfine coupling increases to 178 $\times 10^{-4}$ cm^{-1} for the reference planar tetrakis(imidazole) chromophore, bis[2,2′-bis(5-phenyl-2-imidazolyl)propane]Cu(II) diperchlorate (**15**), that has no apical ligation.[66]

Table VIII. X-Band EPR Parameters

system	$g_{\perp}$	$g_{\parallel}$	$A_{\parallel}^{Cu}$ [f]	ref
$CuL_2(ClO_4)_2$ [a]	2.04	2.26	130	g
$CuL_2(ClO_4)_2$ [b]	2.02	2.25	147	g
$CuL_2(BF_4)_2$ [b]	2.02	2.24	146	g
$Cu(Me_2L)_2(BF_4)_2$ [b]	2.03	2.26	148	g
Cu(II)/$ZnL_2(ClO_4)_2$ [c]	2.06	2.32	118	g
bis[2,2-bis(5-phenyl-2-imidazolyl)propane]-$Cu^{II}(ClO_4)_2$ [d]	2.08	2.26	178	66
Cu(II)/Zn(II) superoxide dismutase [e]	2.02 (g_x) 2.118 (g_y)	2.316 (g_z)	116 (A_z)	13
hemocyanin, half-met nitrite	2.096	2.302	125	67
tyrosinase, half-met nitrite	2.078	2.296	131	67

[a] Powder spectra taken at 80 K and ambient temperature. [b] Spectra recorded at 80 K of 5.0 mM glassed acetonitrile solutions of the salt. [c] Powder spectra taken at 80 K of $ZnL_2(ClO_4)_2 \cdot 3CH_3CH_2OH$ doped nominally at the 3% level with Cu(II). The Zn(II) complex is isostructural with the Co(II) and Ni(II) complexes 6 and 7. Lattice constants for $ZnL_2(ClO_4)_2 \cdot 3CH_3CH_2OH$ at 298 K are a = 27.26(1) Å, b = 13.021(3) Å, c = 16.18 (1) Å, β = 125.44 (5)°. [d] Spectra recorded at 80 K of a 5 mM glassed methanol solution. [e] Spectrum of superoxide dismutase with Cu(II) doped into the Zn(II) site. [f] Units, cm$^{-1} \times 10^4$. [g] This work.

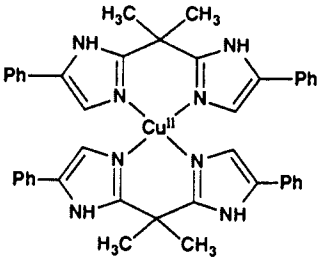

15

The EPR spectrum of the Cu(II)-doped ZnL_2 complex is very similar to that observed for Cu(II) doped into the distorted tetrahedral Zn(II) site of superoxide dismutase, in which N_3O ligation is provided by two histidine imidazole N atoms, the N atom from a bridging imidazolate group, and an aspartate O atom.[15b] The EPR spectrum of the doped complex is also similar to those of the half-met nitrite and other derivatives of hemocyanin and tyrosinase[67] whose active site structures have not yet been determined by X-ray crystallography. The ligand field (LF) absorptions exhibited by these derivatives also are similar to those observed for **5** (see below). Therefore, an alternative D_{2d}, four-coordinate formulation of the Cu(II) active site geometry in these Met derivatives seems worthy of consideration.

5. Electronic Structural Results. Electronic spectra of the ligand **3** and of its 2:1 complexes with Cu(II), Ni(II), and Co(II) are presented in Figures 7–10 and summarized in Table IX. The ligand does not exhibit electronic absorptions at wavelengths longer than 300 nm. Below 300 nm, several intense absorptions are observed (Figure 7) whose features resemble those reported for its biphenyl and phenylimidazole substructures.[68] We have noted elsewhere that the UV absorptions of simple monodentate imidazoles are not changed much by complexation to Cu(II) ions.[23] The same situation apparently obtains for **3**. However, in contrast

(64) (a) Goetz, A. G.; Denney, D. Z.; Potenza, J. A. *J. Phys. Chem.* **1979**, *83*, 3029. (b) Gerardi, G. J.; Potenza, J. A. *J. Phys. Chem.* **1981**, *85*, 2034.

(65) Penfield, K. W.; Gewirth, A. A.; Solomon, E. I. *J. Am. Chem. Soc.* **1985**, *107*, 4519.

(66) Prochaska, H. J.; Schwindinger, W. F.; Schwartz, M.; Burk, M. J.; Bernarducci, E.; Lalancette, R. A.; Potenza, J. A.; Schugar, H. J. *J. Am. Chem. Soc.* **1981**, *103*, 3446.

(67) Himmelwright, R. S.; Eickman, N. C.; LuBien, C. D.; Lerch, K.; Solomon, E. I. *J. Am. Chem. Soc.* **1980**, *102*, 7339, and references cited therein.

(68) Simons, W. W., Ed. *The Sadtler Handbook of Ultraviolet Spectra*; Sadtler Research Laboratories: Philadelphia, PA 19104; 1979; Vol. 1. *UV Atlas of Organic Compounds*; Plenum Press: New York, 1971; Vol. V.

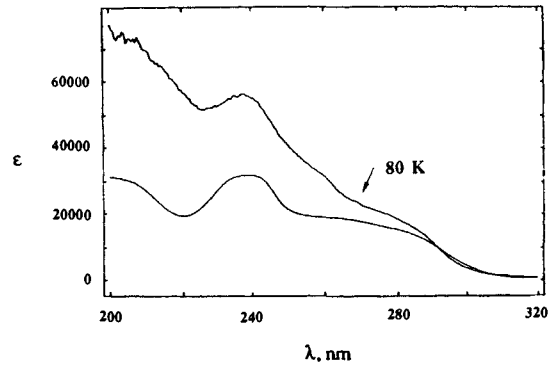

Figure 7. Electronic spectrum of a 0.55 mM solution of **3** in ethanol at 298 K and 80 K.

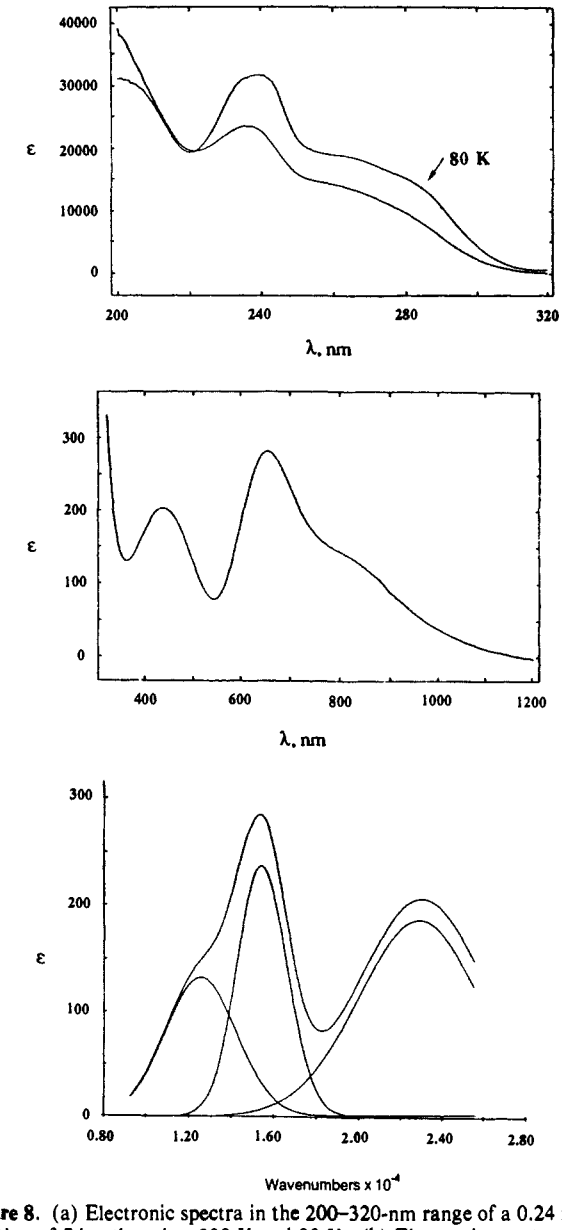

Figure 8. (a) Electronic spectra in the 200–320-nm range of a 0.24 mM solution of **5** in ethanol at 298 K and 80 K. (b) Electronic spectrum in the 300–1200-nm range of a 2.3 mM solution of **5** in ethanol at 298 K. (c) Gaussian deconvolution of the visible–near-UV absorption envelope in (b).

to the ligand-localized absorptions of simple imidazoles, those of **3** span a broader range and are sufficiently intense to obscure the imidazole → M(II) charge-transfer absorptions of its complexes over the UV region. For these reasons, the UV spectra of the complexes of **3** with Cu(II), Ni(II), and Co(II) are not appreciably changed from those of the free ligand.

Table IX. Summary of Electronic Spectral Results[a] and Assignments

compound	λ, nm	ν, cm^{-1}	ε	assgnmt
5, Cu(II) complex	235	42 500	48 000	ligand
	280	35 700	12 000	ligand
	440	22 700	260	π(imH) → Cu(II) LMCT
	650	15 400	260	LF
	800	12 500	120	LF
	457[b]	21 900		
	640[b]	15 600		
	800[b]	12 500		
	450[c]	22 200		
	630[c]	15 900		
	800[c]	12 500		
6, Ni(II) complex	350	28 600	800	π(imH) → Ni(II) LMCT
	470	21 300	140	LF
	640	15 600	85	LF
	770	13 000	30	LF
7, Co(II) complex	310	32 300	900	π(imH) → Co(II) LMCT
	520	19 200	470	LF
	590	17 000	600	LF

[a] Spectra of the perchlorate salts in ethanol solution at 298 K except where noted. [b] Glassed ethanol solution at 80 K. [c] Mineral oil mull at 80 K.

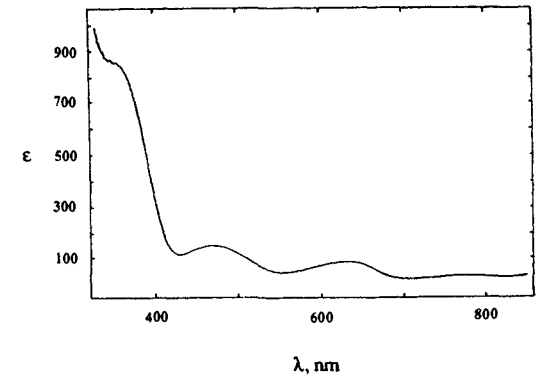

Figure 9. Electronic spectrum of a 2.4 mM solution of **6** in ethanol at 298 K.

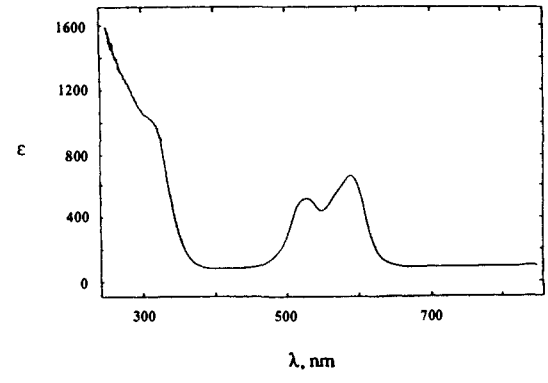

Figure 10. Electronic spectrum of a 2.4 mM solution of **7** in ethanol at 298 K.

Solution spectra of the Cu(II) complex **5** in ethanol at 298 K are presented in Figure 8 along with the Gaussian deconvolution of the overlapping three lowest energy absorptions. For clarity of presentation, we have chosen not to add the base-line correction to the simulated spectra; the corrected simulated spectra are essentially congruent with the observed spectra. Bands having the same energies and intensities are obtained after deconvolution of the corresponding spectra obtained in acetonitrile and acetone solutions. Better resolved spectra (not shown) are exhibited by ethanol glasses of **5** at 80 K. The absorptions at 440 and 650 nm narrow somewhat and exhibit the modest shifts noted in Table IX. The spectra of **5** dispersed in a mineral oil mull exhibit

essentially the same absorption maxima as the solution spectra of **5**. As noted above, the EPR spectra of neat, polycrystalline **5** and glassed solutions of **5** in these three solvents are also similar. *These combined spectroscopic data indicate that the structure of the solution complexes exhibits little variation with solvent and that the solid-state structure of* **5** *must be well-conserved in the solutions studied.* For Cu(II)–imidazole complexes, three LMCT absorptions are expected; these originate from the sp^2 nitrogen lone pair (n, highest in energy) and from two π-symmetry ring orbitals, π_2, the SHOMO, and π_1, the HOMO.[23] We assign the absorption of the Cu(II) complex **5** at 22 700 cm^{-1} (ϵ = 260) as the lowest energy π(imH) → Cu(II) LMCT absorption. Its energy exceeds the upper limit of 20 000 cm^{-1} appropriate for a ligand field absorption of a tetrakis(imidazole)Cu(II) chromophore. The maximum ligand field splitting and thus highest energy LF absorption is expected for a planar $Cu^{II}N_4$ unit whose ligation is supplied by electron-rich imidazoles. This situation obtains for the tetrakis(1,4,5-trimethylimidazole)Cu(II) complex having nonligating perchlorate counterions.[44] Since the CuN_4 unit of **5** shows substantial tetrahedral distortion from the limiting D_{4h} geometry, its LF absorptions must be appreciably red-shifted. We assign the bands at 15 400 (ϵ = 260) and 12 500 cm^{-1} (ϵ = 120) as LF absorptions. Absorptions in this spectral region are exhibited by other tetrahedrally distorted $Cu^{II}N_4$ chromophores.[18,69] The respective widths at half-height of the deconvoluted LF bands are 2950 and 2500 cm^{-1}; the charge-transfer band at 22 700 cm^{-1} is apparently broader (6400 cm^{-1}). For a D_{2d} Cu(II) complex, three LF absorptions are expected, which increase to four upon distortion to C_2 or D_2 symmetry.[70] No additional LF absorptions occur in the 10 000–6600-cm^{-1} region of the spectra for **5** in glassed ethanol at 80 K. Only relatively sharp absorptions, characteristic of vibrational overtones, are present.

To estimate the EPR parameters of the Cu(II) complex **5** in the limit of D_{2d} flattening to a planar CuN_4 unit, we have investigated the spectroscopic reference complex tetrakis(2-phenylimidazole)Cu(II) diperchlorate. The electronic spectra of this complex include a LF band at 16 600 cm^{-1} (ϵ = 70) and π_1(imH) and π_2(imH) → Cu(II) LMCT bands at 26 300 (ϵ = ca. 2400) and 29 400 cm^{-1} (ϵ = ca. 1600), respectively. These LMCT absorptions are red-shifted by ~3000 cm^{-1} relative to those exhibited by tetrakis Cu(II) complexes of alkylated imidazoles.[23,44] Possibly, electronic interactions between the imidazole and biphenyl portions of ligand **3** have increased the energies of the imidazole frontier orbitals, thus allowing the imH → Cu(II) LMCT absorptions to occur at lower energies. We have reported effects of this type in the LMCT spectra of the Cu(II) complexes of 2,2′-biimidazoles.[71]

The effect of the tetrahedral twist in the Cu(II) complex **5** is to reduce the intensity of the lowest energy imH → Cu(II) LMCT band considerably and to cause it to red-shift by 3600 cm^{-1} relative to the corresponding absorption of the reference complex. Some of the red-shift must result from the lowering in energy of the Cu(II) d vacancy. Other contributions to this result presumably include the differences in ligand–ligand repulsions and in the many electron reorganization effects that have been noted for the Cl^- → Cu(II) LMCT absorptions of D_{4h} and D_{2d} $CuCl_4^{2-}$ complexes.[72] Finally, we note that the UV absorption edge of the ligand **3** obscures the position of the expected π_2(imH) → Cu(II) LMCT absorption.

The approximate order of magnitude decrease in the extinction coefficient of the π_1(imH) → Cu(II) LMCT absorption exhibited by the Cu(II) complex **5** relative to the planar reference complex can be understood from the EPR and structural results. The EPR studies show that both complexes have $(d_{x^2-y^2})^1$ ground states. The overlap between the Cu(II) d vacancy and the upper occupied imidazole π orbitals is not expected to be particularly good in either complex. However, the σ-symmetry imidazole lone pairs overlap optimally with the Cu(II) d vacancy in the reference complex and thus allow the π_1- and π_2-imH LMCT absorptions to acquire intensity by stealing from highly allowed in-plane polarized n(imH) → Cu(II) absorptions. The tetrahedral twist present in **5** must reduce the overlap between the d vacancy and the four imidazole lone pairs. In our view, this strongly reduces the borrowed intensity of the π_1(imH) → Cu(II) LMCT absorption. Reduced electronic coupling of the d vacancy to the imidazole ligand in **5** may also be help account for its sluggish self-exchange redox reaction.

The electronic spectral results for **5** may be compared with those reported for several Cu(II)-containing metalloprotein active sites. The low intensity and the observed energy of the π_1(imH) → Cu(II) LMCT absorption are reminiscent of the weak near-UV absorptions of plastocyanin that have been the subject of polarized single-crystal spectra studies.[65] In particular, the protein absorption at 21 390 cm^{-1} exhibits a polarization ratio consistent with its assignment as imH → Cu(II) LMCT. While the energy of imH → Cu(II) LMCT has been reasonably well estimated by studies of model systems,[23] the weakness of this absorption could not be duplicated experimentally until a suitable, approximately tetrahedral model became available for study.

Superoxide dismutase (SOD), with Cu(II) doped into the distorted tetrahedral Zn(II) site, shows a band at 26 500 cm^{-1} (ϵ = 250) that has been assigned as π(imH) → Cu(II) LMCT.[13] In native SOD, with Cu(II) in a distorted five-coordinated environment, the lowest energy π(imH) → Cu(II) LMCT absorption occurs at 29 500 cm^{-1} (ϵ = 250).[13] Thus, the energy of the π(imH) → LMCT absorption in **5** compares more favorably to that of the protein with copper in a pseudotetrahedral site. We note also that the EPR parameters and LF absorptions of **5** closely resemble those reported for the nitrite and various other derivatives of half-met hemocyanin and tyrosinase.[67,73] Apparently, these spectroscopic features of flattened D_{2d} Cu(II) can mimic those of typical tetragonal five-coordinate chromophores, increasing the uncertainty of structural assignments made solely on these spectroscopic grounds.

The absorption spectrum of **7** (Figure 10) shows a broad envelope in the 480–630-nm region (ca. 16 000–21 000 cm^{-1}) that consists of at least three overlapping bands; a fourth, higher energy band is located at 310 nm (32 300 cm^{-1}). The intensities and positions of the bands in the low-energy envelope (Table IX) are similar to spectral features observed for the LF transitions of tetrahedral $Co^{II}N_4$ complexes such as $Co(NH_3)_4^{2+}$, which shows absorption maxima at 16 000, 18 000, and 19 200 cm^{-1},[74] and $Co^{II}(1,2\text{-}Me_2imH)_4$, which shows LF transitions at 17 000 (ϵ = 570), 17 500 (ϵ = 550), and 18 900 cm^{-1} (ϵ = 330).[75] The high-energy absorption is assigned as π(imH) → Co(II) LMCT, by analogy to $Co^{II}(1,2\text{-}Me_2imH)_4$ and $Co^{II}(1,2,4\text{-}Me_3imH)_4$, for which bands at 33 900 (ϵ = 400) and 32 200 cm^{-1} (ϵ = 860), respectively, have been so assigned.[75] As with the Cu(II) complex above, the spectrum of the Co(II) complex **7** exhibits similarities to that of SOD with Co(II) doped into the Zn(II) site. For Co(II)-doped SOD with the native Cu(II) site vacant, LF transitions have been reported[76] at 17 150, 17 730, and 18 520 cm^{-1}; with Ag(I) in the native copper site, the corresponding values are 17 150, 17 800, and 18 900 cm^{-1}.[77]

The absorption spectrum of the Ni(II) complex **6** (Figure 9), the first structurally characterized complex with a pseudotetrahedral $Ni^{II}N(imH)_4$ chromophore, reveals bands at 28 600, 21 300, 15 600, and 13 000 cm^{-1} (Table IX). Single-crystal spectra have

(69) Dudley, R. J.; Hathaway, B. J.; Hodgson, P. G. *J. Chem. Soc., Dalton Trans.* **1972**, 882.
(70) Lever, A. B. P. *Inorganic Electronic Spectroscopy, 2nd ed.*; Elsevier: New York; 1984; p 555.
(71) Bernarducci, E. E.; Bharadwaj, P. K.; Lalancette, R. A.; Krogh-Jespersen, K.; Potenza, J. A.; Schugar, H. J. *Inorg. Chem.* **1983**, *22*, 3911.
(72) Dejardins, S. R.; Penfield, K. W.; Cohen, S. L.; Musselman, R. L.; Solomon, E. I. *J. Am. Chem. Soc.* **1983**, *105*, 4590.
(73) Westmoreland, T. D.; Wilcox, D. E.; Baldwin, M. J.; Mims, W. B.; Solomon, E. I. *J. Am. Chem. Soc.* **1989**, *111*, 6106.
(74) Muller, A.; Christophliemk, P.; Tossidis, I. *J. Mol. Struct.* **1973**, *15*, 289.
(75) Schugar, H. J. In *Copper Coordination Chemistry: Biochemical and Inorganic Perspectives*; Karlin, K. D., Zubieta, J., Eds.; Adenine Press: Guilderland, NY, 1983; p 43.
(76) Fee, J. A. *J. Biol. Chem.* **1973**, *248*, 4229.
(77) Beem, K. M.; Richardson, D. C.; Rajagopalin, K. V. *Biochemistry* **1977**, *16*, 1930.

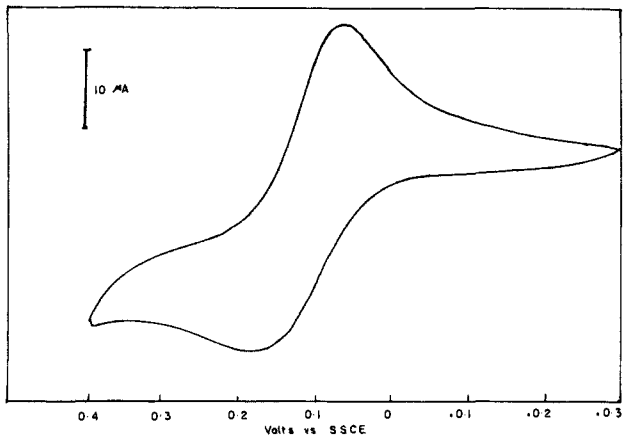

Figure 11. Cyclic voltammogram (in CH_3CN with 0.1 M Et_4NBF_4, Pt electrode, scan rate 50 mV s^{-1}) of a 2.5 mM solution of **5** at 23 (1) °C.

been reported for the low-spin $S = 0$ Ni^{II}(1,2-dimethylimidazole)$_4$·$2ClO_4$ complex, which is known to be square planar.[78] In that complex, the absorption at 35 100 cm^{-1} (ϵ = 440) was assigned as π_1(imH) → Ni(II) LMCT while a band at 22 000 cm^{-1} (ϵ = 130) was assigned as a LF transition.[75] For the pseudotetrahedral Ni(II)-doped Zn(1,2-dimethylimidazole)$_2Cl_2$ system, the π_1(imH) → Ni(II) LMCT band was observed at 30 800 cm^{-1} while LF bands in the polarized single-crystal spectra occurred at 17 800, 16 300, 11 000, 10 600, and 8200 cm^{-1}.[77,79] By analogy, we assign the band at 28 600 cm^{-1} as π_1(imH) → Ni(II) LMCT and the lower energy bands to d–d transitions. The present results suggest a red-shift of ca. 6500 cm^{-1} in the π_1(imH) → Ni(II) LMCT band in going from a planar to an approximately tetrahedral $Ni^{II}N(imH)_4$ chromophore. For Ni(II)-substituted azurin and Ni(II)-substituted stellacyanin, πN(His) → Ni(II) LMCT transitions from the histidine imidazoles were reported at 28 200 cm^{-1} (ϵ = 1530) and 29 900 cm^{-1} (ϵ = 1600);[80] these values are close to that for **8** and are consistent with pseudotetrahedral environments for Ni(II) in the substituted proteins.

6. Electrochemistry. A 2.5 mM solution of **5** in acetonitrile showed a reversible cyclic voltammetry wave at a potential $E_{1/2}$ = +0.11 (1) V vs SSCE and a scan rate of 50 mV s^{-1} (Figure 11); within experimental error, the peak separation was equal to that of the Fc/Fc^+ standard in the same solution. These waves correspond to the reduction of **5** to **8** and the oxidation of **8** to **5**. Reversibility for this redox process was anticipated based on the crystallographic and NMR data presented above and implies that the cations in **5** and **8** retain their solid-state geometry in solution to a large degree. Other examples of reversible or quasi-reversible Cu(I)/Cu(II) redox pairs with well-documented equivalent ligation in the reduced and oxidized forms are rare. They include three structurally related, five-coordinate Cu(I)/Cu(II) complexes[26] with the pentadentate N ligands $(py)_2$DAP, $(imidH)_2$DAP, and $(imidR)_2$DAP, **16–18**, as well as the cop-

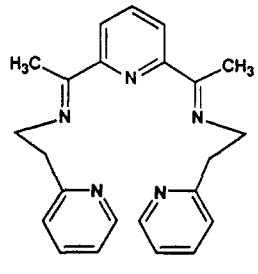

16

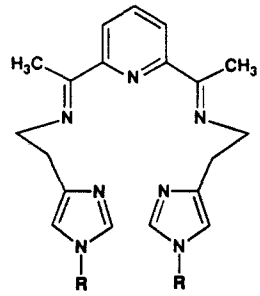

17, R = H
18, R = *p*-Me(C_6H_4)CH_2

(78) Potenza, M. N.; Potenza, J. A.; Schugar, H. J. *Acta Crystallogr.* **1988**, *C44*, 1201.
(79) Bharadwaj, P. K.; Potenza, J. A.; Schugar, H. J, unpublished results.
(80) Lum, V.; Gray, H. B. *Isr. J. Chem.* **1981**, *21*, 23.

Table X. Reduction Potentials, $E_{1/2}$ vs SSCE (V), for Cu(II)/Cu(I) Pairs

complex	$E_{1/2}$	ligand set	solvent	ref
$[Cu(imidH)_2DAP]^{n+}$	−0.27	N_5	CH_3CN	26
$[Cu(imidR)_2DAP]^{n+}$	−0.26	N_5	CH_3CN	26
$[Cu(py)_2DAP]^{n+}$	−0.14	N_5	CH_3CN	26
$[CuL_2]^{n+}$	+0.11	N_4	CH_3CN	this work

per-containing protein plastocyanin.[7] We note that, while comparison of electrochemical results from different laboratories is difficult owing to differences in electrodes, cells, solvent, and other aspects of system configuration, measurements for the DAP systems and ours were made with a similar electrode configuration in the same solvent and can reasonably be compared. The results (Table X) show that the $E_{1/2}$ value for the **5**/**8** redox pair is substantially more positive than those of the five-coordinate Cu(I)/Cu(II) complexes, in harmony with the small LF energy of tetrahedral Cu(II) relative to those for typical five- and six-coordinate Cu(II) geometries.

Conclusions

We have probed the structural, spectroscopic, and electron self-exchange properties of several first-row transition-metal complexes prepared with the novel bidentate ligand L = **3** and its N-methylated derivative **4**. Single-crystal X-ray structure analysis of the perchlorate salts of $Cu^{II}L_2$ (**5**), $Ni^{II}L_2$ (**6**), $Co^{II}L_2$ (**7**), and $Cu^{I}L_2$ (**8**) revealed $MN(imH)_4$ chromophores, each with virtual D_{2d} point symmetry, as indicated by an analysis of the N–M–N angles. Observed MN_2/MN'_2 dihedral angles range from 87.7 (2) to 89.5 (1)°, very close to the value of 90° expected for T_d or D_{2d} point symmetry. Analysis of the structural data shows (1) that the degree of D_{2d} flattening in these pseudotetrahedral complexes is greatest in the Cu(II) complex, followed by the Ni(II), Co(II), and Cu(I) complexes, and (2) that the ligand **3** utilizes steric constraints to exert an unprecedented degree of geometric control of the coordination spheres.

X-band EPR parameters for the Cu(II) complex **5** doped into the isostructural Zn(II) complex are remarkably similar to those for Cu(II) doped into the pseudotetrahedral Zn(II) site of superoxide dismutase. In particular, both the $g_\parallel$ and $A_\parallel^{Cu}$ values are identical within experimental error, and the average of g_x and g_y for the protein is equal to $g_\perp$ for **5**. The UV–vis spectrum of **5** includes a band centered at 22 700 cm^{-1}, which is assigned as π(imH) → Cu(II) LMCT. This band is ca. 3600 cm^{-1} lower in energy and less intense than comparable transitions observed for a reference tetrakis(2-phenylimidazole) complex containing tetragonal $Cu^{II}N_4$ chromophores. It compares more favorably to the values of 25 500 and 21 400 cm^{-1} reported, respectively, for the π(imH) → Cu(II) LMCT transition in Cu(II)-doped Zn(II) superoxide dismutase and in native plastocyanin.

The Ni(II) complex **6** provides the first structurally characterized complex with a pseudotetrahedral $Ni^{II}N(imH)_4$ chromophore. The UV–vis spectrum of **6** includes a band centered at 28 600 cm^{-1}, which is assigned as π(imH) → Ni(II) LMCT and which is red-shifted by approximately 6500 cm^{-1} from comparable transitions observed in square-planar Ni(II) complexes with imidazole ligands. The value of 28 600 cm^{-1} is quite close to those reported for the πN(his) → Ni(II) LMCT transitions in Ni(II)-substituted azurin (28 200 cm^{-1}) and Ni(II)-substituted stellacyanin (29 900 cm^{-1}). Overall, the spectroscopic properties of the pseudotetrahedral complexes prepared in this study appear to mimic quite well those of proteins containing imidazole ligation to metals in distorted tetrahedral environments.

Complexes **5** and **8** are particularly interesting; they provide a nearly tetrahedral $Cu^{I}N_4/Cu^{II}N_4$ redox pair with the same ligands that gives a reversible cyclic voltammetric wave in CH_3CN, and that should be suitable for studying electron self-exchange in a system where ligand and solvent reorganization is expected to be minimal. Attempts to measure the electron self-exchange rate constant k in CH_3CN using line-broadening (T^*_2) and T_1 techniques gave an upper limit for k of 10^2 M^{-1} s^{-1}, a value that is surprisingly small when compared with those for several cop-

per-containing proteins (ca. 10^5–10^6 M^{-1} s^{-1}) or low molecular weight complexes with bidentate or polydentate ligands (10^2–10^7 M^{-1} s^{-1}). Indeed, only water as a ligand is reported to show a self-exchange rate constant significantly smaller than this upper limit. One possibility for the small value of k in the present system is the lack of an effective orbital pathway coupling the unpaired electron in the Cu(II) $d_{x^2-y^2}$ orbital to the appropriate electron donor oribtal in the Cu(I) complex.

Acknowledgment. This research was supported by the NSF (Grant CHE 84-17548), the David and Johanna Busch Foundation, and the NIH (Instrumentation Grant 1510 RRO 1486 O1A). We thank Dr. R. Mobashar for help with the electrochemical measurements and Profs. S. Isied, E. Solomon, and A. M. Yacynych for helpful discussions. We thank Dr. B. Toby for help in constructing the digitized EPR data aquisition system, J. Bumby for assistance in measuring and simulating EPR spectra, and J. Westbrook for local revisions of the EPR simulation program that was furnished by the Illinois ESR Research Center, NIH Division of Research Resources Grant No RR01811.

Note Added in Proof. Reduced coupling of the Cu(II) d vacancy to the imidazole ligands in another pseudotetrahedral complex, Cu(II)-doped $ZnCl_2$-(1,2-dimethylimidazole)$_2$, has been observed by single-crystal EPR studies (Gewirth, A. A.; Cohen, S. L.; Schugar, H. J.; Solomon, E. I. *Inorg. Chem.* **1987**, *26*, 1133) and by single-crystal electron spin-echo envelope modulation studies (Colenari, M. J.; Potenza, J. A.; Schugar, H. J.; Peisach, J., submitted for publication). This latter study reveals that the SHF coupling constants of both the directly ligated and remote imidazole nitrogens are approximately half of those exhibited by planar Cu(II) tetraimidazole complexes.

Supplementary Material Available: Tables of atomic coordinates, anisotropic and isotropic thermal parameters, and bond distances and angles for **5–8** (39 pages); observed and calculated structure factors for **5–8** (86 pages). Ordering information is given on any current masthead page.

A Total Synthesis of Racemic Paulownin Using a Type II Photocyclization Reaction

George A. Kraus* and Li Chen

Contribution from the Department of Chemistry, Iowa State University, Ames, Iowa 50011.
Received October 3, 1989. Revised Manuscript Received November 13, 1989

Abstract: The lignan paulownin was prepared in a seven-step route from piperonal. The key step was a type II photocyclization reaction wherein two of the four stereogenic centers were introduced.

Photochemical reactions have been employed for the construction of a wide range of natural products.[1] Smith,[2] Crimmins,[3] and Winkler[4] have made effective use of the 2 + 2 cycloaddition reaction for the synthesis of terpenes and alkaloids. Mariano[5] has studied electron transfer cyclizations of amino ketones, providing novel strategies for the synthesis of fused and spirocyclic compounds. Schultz[6] has harnessed the photochemical rearrangements of cyclohexadienones, generating clever and direct syntheses of cyclopentenones and other useful synthetic intermediates. In contrast, the hydrogen atom abstraction–cyclization chemistry, often termed the type II photocyclization, has been almost unused in natural products synthesis. One notable exception is the elegant use of this reaction by Paquette to create the cyclobutane ring in punctatin.[7] Photoenolization, a related reaction, has been used by Oppolzer and others for alkaloid synthesis.[8] In this article we report the first total synthesis of paulownin,[9] a novel lignan. The key step in the synthesis is a type II photocyclization for the stereoselective formation of one of the heterocyclic rings.

The photophysical basis of the type II photocyclization reaction has been well studied, most notably by Wagner and Scaiano.[10]

Scheme I

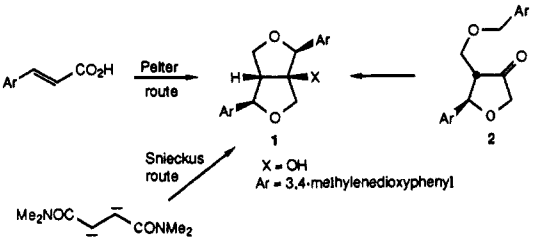

They have demonstrated that an n–π^* triplet state is involved in the type II photocyclizations of diaryl and aryl alkyl ketones. They also reported that subtle conformational effects can profoundly influence product distributions. The type II photocyclization reactions of aryl glyoxylates have been rigorously examined by Pappas[11] and by Lappin[12] (eq 1). Pappas discovered a dramatic solvent effect on the stereochemistry of the cyclization.

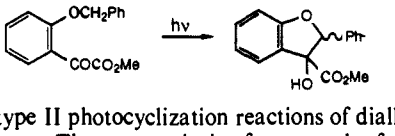

(1)

Studies of type II photocyclization reactions of dialkyl ketones are less common. The vast majority focus on the formation of cyclobutanols.[13] Indeed, unless the 1,5-hydrogen atom abstraction pathway is blocked, it will be the predominant one. Paquette made

(1) Wender, P. *Selectivity—A Goal for Synthetic Efficiency*; Bartman, W., Trost, B., Eds; Springer-Verlag: New York, 1984; p 335.
(2) Smith, A. B.; Boschelli, D. *J. Org. Chem.* **1983**, *48*, 1217.
(3) Crimmins, M. D. *Chem. Rev.* **1988**, *88*, 1453.
(4) Winkler, J. D.; Hershberger, P. M. *J. Am. Chem. Soc.* **1989**, *111*, 4852.
(5) Kavash, R. W.; Mariano, P. S. *Tetrahedron Lett.* **1989**, *30*, 4185 and references therein.
(6) Schultz, A. G.; Lavieri, F. P.; Macielag, M.; Plummer, M. *J. Am. Chem. Soc.* **1987**, *109*, 3991.
(7) Pacquette, L. A.; Sugimura, T. *J. Am. Chem. Soc.* **1986**, *108*, 3841.
(8) Quinkert, G.; Weber, W. D.; Schwartz, U.; Stark, H.; Baier, H.; Duerner, G. *Liebigs Ann. Chem.* **1981**, 2335. Oppolzer, W.; Keller, K. *Angew. Chem., Int. Ed. Engl.* **1972**, *11*, 728.
(9) Takahashi, K.; Nakagawa, N. *Chem. Pharm. Bull.* **1966**, *14*, 641.
(10) Wagner, P. J. *Acc. Chem. Res.* **1989**, *22*, 83 and references therein.
(11) Pappas, S. P.; Pappas, B. C.; Blackwell, J. E. *J. Org. Chem.* **1967**, *32*, 3066.
(12) Lappin, G. R.; Zannucci, J. S. *J. Org. Chem.* **1971**, *36*, 1808.
(13) Coyle, J. D. *Photochemistry in Organic Synthesis*; Royal Society of Chemistry: London, 1986; Chapter 4.

0002-7863/90/1512-3464$02.50/0